Journal of
Geotechnical and Transportation Engineering

JGTTE

ISSN: 2379-8769| www.jgtte.com

July 2018
Volume 4 | Issue 1

Journal of Geotechnical and Transportation Engineering

Aim and Scope

The Journal of Geotechnical and Transportation Engineering (JGTTE) covers the broad areas of practice known as geotechnical engineering and transportation engineering. The journal intends to provide a platform for publication of the high-quality researcher in common areas among the geotechnical and transportation engineering. JGTTE focuses on the papers that have applications in either of these fields, with emphasis on theoretical aspects.

The specific topics that are covered by the journal are road and highway design, sub layers of railroad, geosynthetic reinforced ground, retaining structures, soil dynamics and foundations, engineering behavior of soil and rock, site characterization, slope stability, dams, rock engineering, earthquake engineering, environmental impacts of geotechnical and transportation engineering, geosynthetics, computer modeling, groundwater monitoring and restoration, geomechanics, planning, design, construction, maintenance, and operation of air, highway, rail, and urban transportation, pavement maintenance and performance, management of roads, bridges, and transit systems, traffic management technology, railway engineering and economics. Authors are also encouraged to submit papers on new and emerging topics within the general discipline of geotechnical and transportation engineering. Experimental papers are also welcomed, especially the ones with a clear and significant potential for practical application. Practice-oriented papers and case studies are particularly welcomed and encouraged.

Publisher:
Journal of Geotechnical and Transportation Engineering

July 2018
Volume 4 | Issue 1

Instructions for Authors

1. Format the Paper

The paper should have the following structure:
• A Title, which adequately describes the content of the paper and should not exceed 80 characters;
• An Abstract, which should be viewed as a mini version of the paper and should not exceed 350 words. The Abstract should state the principal objectives and the scope of the investigation and the methodology employed; it should also summarize the results and state the principal conclusions;
• A maximum of 6 keywords, which should be written immediately after the abstract;
• An Introduction, which should provide a review of recent literature and sufficient background information to allow the results of the paper to be understood and evaluated;
• A Theoretical and Experimental section, which should provide details of the theory and the experimental set-up and the methods used to obtain the results;
• A Results and discussion section, which should clearly and concisely present the data, using figures and tables where appropriate; It should also describe the relationships shown and the generalizations made possible by the results and discuss the significance of the results, making comparisons with previously published work
• Conclusions, which should present one or more conclusions that have been drawn from the results and subsequent discussion;
• A list of References, which comprises all the references cited in the text, and vice versa.

Submission Requirements:
• Figures and tables must be included in the text of the manuscript.
• Use a normal, plain font (e.g., 9-point Times Roman) for text and single line-spacing.
• Insert continuous line numbering.
• The submitted manuscript should not exceed 20 pages. Results may be shown in tables or figures, but not in both of them.

2. Units and Abbreviations

Standard SI symbols and abbreviations should be used in the text, tables and figures. Imperial units can also be used only if they are accompanied with SI equivalents in brackets. Symbols for physical quantities in the text should be written in Italics (e.g. v, T, etc.). Symbols for units that consist of letters should be in plain text (e.g. Pa, m, etc.). All abbreviations should be spelt out in full on first appearance.

3. Figures and Tables

Figures must be cited in consecutive numerical order in the text and referred to in both the text and the caption as Fig. 1, Fig. 2, etc. Figures may be saved in any common format, e.g. BMP, JPG, GIF. When labelling axes, words should be used rather than symbols. Axes should not be labeled only with units. Multi-curve graphs should have individual curves marked with a symbol; the meaning of the symbol should be explained in the figure caption. The figures should have a high quality and be clear in black and white. A color version of the accepted papers will be available electronically. The printed version will be only in black and white and the authors will be required additional charges if they are interested in the color print. Tables must also be cited in consecutive numerical order in the text and referred to in both the text and the caption as Table 1, Table 2, etc. The use of names for quantities in tables should be avoided if possible: corresponding symbols are preferred. In addition to the physical quantity, e.g. t (in Italics), units (normal text), should be presented within brackets. Any footnotes should be indicated by the use of the superscript.

4. Author Information

The following information about the authors should be enclosed with the paper: names, complete postal addresses, telephone and fax numbers and E-mail addresses. Indicate the name of the corresponding author. A 2x2 professional picture of the authors.

5. Acceptance of Papers and Copyright

The Editors-in-Chiefs of the JOURNAL OF GEOTECHNICAL AND TRANSPORTATION ENGINEERING reserves the right to decide whether a paper is acceptable for publication, to obtain peer reviews for the submitted papers, and, if necessary, to require changes in the content, length or language. On publication, the copyright for the paper shall pass to the Journal of Geotechnical and Transportation Engineering. The JGTTE must be stated as a source in all later publication.

6. Submit a Paper

To submit a paper, please prepare your paper according to the provided instructions and email the full paper with the figures and tables in the text to submission@jgtte.com .

For more information and sample paper, please visit the website: www.jgtte.com

Journal of Geotechnical and Transportation Engineering

Copyright

Volume 4 | Issue 1

Proof Reader:

Sue Mahmood

Strayer University, USA

Technical Manager:

Hesam Shabaniverki

Washington, D.C., USA

JGTE

July 2018

Volume 4 | Issue 1

Journal of Geotechnical and Transportation Engineering
Volume 4 | Issue 1
Matric Suction, Swelling and Collapsible Characteristics of Unsaturated Expansive Soils
Pandya and Sachan
Received 5/2/2018 Accepted 6/1/2018
Published 7/1/2018
Corresponding Author:
Saloni Pandya;
pandya_saloni@iitgn.ac.in
www.jgtte.com

Matric Suction, Swelling and Collapsible Characteristics of Unsaturated Expansive Soils

Saloni Pandya
PhD Scholar, Civil Engineering, Indian Institute of Technology Gandhinagar, India
E-mail: pandya_saloni@iitgn.ac.in

Ajanta Sachan
Associate Professor, Civil Engineering, Indian Institute of Technology Gandhinagar, India.
E-mail: ajanta@iitgn.ac.in

Abstract

Unsaturated expansive soils are recognized as one of the most problematic soils owing to its swelling-shrinkage characteristics. The presence of such soils in highway/railway embankments, slopes and earthen dam sites manifests various critical issues during and after the construction of structures. The current research aims on the evaluation of the suction, swelling and collapsible characteristics of four expansive soils possessing different expansiveness and mineralogical composition. A series of constant volume swell pressure, double-oedometer and in-contact filter paper tests were performed on four different expansive soils to acquire swelling pressure, collapse potential and matric suction at different degree of saturation. Swelling pressure, collapse potential and matric suction of all expansive soils degraded substantially with increment in the degree of saturation. The results revealed significant impact of magnitude of matric suction on volumetric deformation (swell and collapse) behavior of expansive soils. Swelling and collapse potential were observed to be higher for the expansive soils with larger matric suction. Higher matric suction governed the water intake within interlayer spacing of the Montmorillonite mineral present in expansive soil, which contributed to higher crystalline swelling response. Larger collapse potential indicated development of larger localized deformations within the soil mass owing to higher matric suction.

Keywords: Expansive, Unsaturated, Matric suction, Swell Pressure, Collapse Potential

1. Introduction

Natural soils (Black cotton soils) possessing tendency to swell (in the presence of water) and shrink (in the absence of water) are referred as expansive soils. Such soils in unsaturated state (S_r < 100%) experiences severe swelling and shrinkage owing to transient variation in degree of saturation of soil mass in the active zone/ vadose zone subjected to climatic cycles. Formation of expansive soils is caused due to chemical weathering of basaltic rocks. The lower amount of precipitation, high condensation due to high temperature and fluctuating drying & wetting cycles are accountable for predominantly leaching and chemical weathering of rocks. Expansive soil covers large portion of earth surface usually in the semi-arid and arid environmental regions (Nalbantoglu and Gucbilmez, 2001). Around 20% of regions in India comprises of shrinkage-swelling (expansive) soils. Expansive soils are found in several parts of Gujarat, Uttar Pradesh, Andhra Pradesh, Karnataka, western Madhya Pradesh and Maharashtra (Verma and Maru, 2013). The critical problem related to expansive soils was found to be associated with induced deformations. Developed deformations in expansive soils were reported to be severely greater than the elastic deformations, which could not be anticipated by classical elastic and plastic theory (Nelson and Miller, 1997). Extent of volumetric deformation would cause severe upheaving and large cracks in embankments & pavements; destruction to the floor slabs; basement buckling due to increased lateral stresses; concrete and steel plinths failure; deterioration of water pipelines; and damages to retaining walls etc. (Charlie et al. 1984). These detrimental volumetric changes would be governed by clay mineralogy, plasticity, soil-water chemistry, depth of ground water table, vegetation cover, temperature, amount of moisture variation over space and time, permeability, soil profile etc. (Nelson and Miller, 1997; Houston et al. 2009). Rapid urbanization has triggered the growth of potential sources of water content upsurge within soil strata; broken sewer and water lines, poor surface drainage, ground water recharge, landscape irrigation, damming due to fill/cut construction, cessation of pumping after building occupation etc. (Houston et al. 2009). Sudden increase of water quantity or overburden stress buildup would cause hydroconsolidation/ collapse of the soil skeleton stimulating excessive damages to the structures and hefty differential settlements. Presence of expansive soils in highway/railway embankments and pavements could lead to detrimental failures owing to swelling followed by collapse response of unsaturated expansive soil due to sudden saturation and vehicular vertical stress. Matric suction would influence the hydro –mechanical behaviour of unsaturated soil (Nowamooz and Masrouri, 2010). Matric suction would control the geometric arrangement of particles within the soil mass, which could induce the volume change behaviour (Swelling and Collapse) within the expansive soil skeleton. The present research focuses on the investigation of the swelling, collapsible and matric suction characteristics of four expansive soils. The effect of mineralogical composition of expansive soils on matric suction, swelling pressure and collapse potential was studied. Both swelling and collapse behaviour of the unsaturated expansive soil were dominated by the amount of matric suction in soil mass at different degree of saturation. Relationship between matric suction of expansive soil with its swelling pressure and collapse potential was also assessed. The role of matric suction governing the mechanism behind swelling and collapsible characteristics of expansive soil were also comprehensively illustrated in the current research.

2. Material properties and specimen preparation

In the current research, four expansive soils (S1, S2, S3 and S4) were collected from Nagpur (Gosikhurd dam site, Maharashtra), Bharuch (Gujarat), Bharuch-Dahej Highway soil (Gujarat) and Chandkheda (Gujarat) respectively. Fig 1. (a) and (b) presents the locations of soil collection sites in political and topographical map of India respectively. Expansive Soils were collected from 0.5m depth to avoid the presence of organic matter on the upper portion of the soil strata. Grain size distribution curves of collected expansive soils are shown in Fig 2. The soil classification, Atterberg limits (*LL*, *PL* and *SL*) and specific gravity (G_S) are presented in Table 1. Differential free swell index (*DFSI*) of Nagpur soil, Bharuch soil, B-D highway soil and Ahmedabad soil were obtained to be 134%, 104%, 70% and 30% respectively. X-Ray diffraction analysis was performed on all four expansive soil specimens to determine their mineralogical compositions. The percentage of Montmorillonite mineral was obtained to be largest for Nagpur soil and lowest for Ahmedabad soil (Table 1). Relationship of Atterberg limits with *DFSI* of four expansive soils is presented in Fig 3. Percentage of Montmorillonite mineral and *DFSI* values indicated Nagpur soil to be most expansive and Ahmedabad soil to be non-expansive in nature.

Moist tamping technique was opted for preparing specimens to perform filter paper, double oedometer and constant volume swell pressure tests. Detailed descriptions regarding the procedure incorporated for moist tamping method was described in Pandya and Sachan (2017a). Specimens were prepared at 1.46 g/cc dry density with different degree of saturation (S_r) values varying from 30% to 97%. Detailed information regarding specimen preparation of different expansive soils is given in Table 2.

Fig 1. Google map representing locations of expansive soils. (a) Location on political map of India, (b) Location on topographical map of India

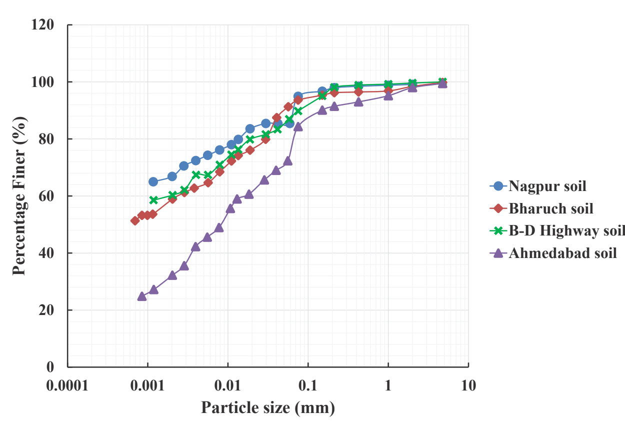

Fig 2. Grain size distribution curves of expansive soils.

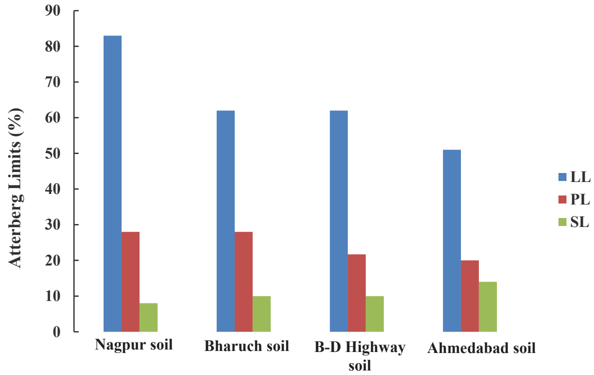

Fig 3. Relationship of Atterberg limits with *DFSI* of expansive soils

3. Experimental program

Matric suction, swell pressure and collapse characteristics of four expansive soils were determined by performing filter paper, constant volume swell pressure and double oedometer tests respectively.

3.1 Matric suction

Filter paper method was employed to determine matric suction for four expansive soils (S1, S2, S3 and S4). In-contact filter paper method covers large range of suction from 10kPa to 100 MPa. Method has been designated as the most efficient, low costing and accurate for measurement of matric suction for all types of soil. Filter paper method was performed as described in ASTM D5298-10 (2013) using Whatman 42 ashless filter paper. Detailed procedure and complete description of methodology of filter paper tests were explained by Pandya and Sachan (2017a). Calibration curve for Whatman 42 (ASTM D5298-10, 2013) was used for determination of matric suction in current study.

3.2 Swell Pressure

Swelling pressure (P_s) can be designated as the pressure exerted by the expansive soil, when change in the volume of soil is restricted. Swelling pressure (P_s) of expansive soils were determined employing constant volume swell pressure tests (Fig 4). In this test, the specimen was prepared in the ring (*d*- 60mm and *h* -20mm) using moist tamping method. The ring was then placed in a thick steel vessel with flat base and wider diameter. The specimen was then attached to the proving ring to restrict volume change (Fig 4). Proving ring was attached to reaction frame with capacity of 1 tonne. After the test setup, the water was poured in the container to allow the specimen saturation. Water penetration inside the specimen instigated swelling in the soil and the pressure exerted by the soil was reflected from proving ring under constant volume conditions. The swelling pressure of the soil was recorded from the proving ring at different time intervals till the reading became constant.

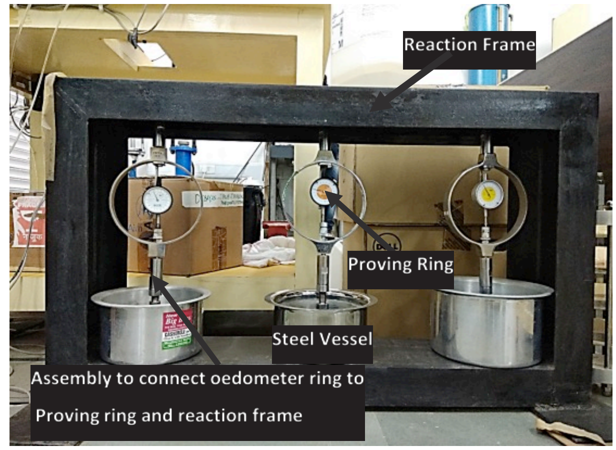

Fig 4. Constant volume swell pressure apparatus

3.3 Collapse potential

Collapse potential indicates the amount of collapse of soil skeleton exposed to sudden inundation or vertical stress application. In the current research, collapse potential (*CP*) of four expansive soils (S1, S2, S3 and S4) were determined by employing double-oedometer test. In the test, two similar compacted (same dry density and water content) specimens of expansive soil were placed in the oedometer mould of two different testing devices. One out of them was loaded under unsaturated conditions and the other one was initially soaked (saturated) for 24 hrs under seating load of 5 kPa. Both the specimens were further loaded sequentially; 10 kPa, 20kPa, 50kPa, 100 kPa, 200kPa, 400 kPa and 800 kPa. Detailed procedure regarding the double oedometer test was presented by Pandya and Sachan (2017b). Each specimen (as-compacted & saturated) was reached at equilibrium under applied vertical stress in 24 hrs, and the specimen was further loaded sequentially. Equilibrium void ratio (after 24 hrs) representing volumetric strain under each vertical stress increment was assessed for both the specimens. Collapse potential of soil was stated as the difference between volumetric strains at a specific vertical stress normalized by initial void ratio of the specimen. It was ascertained using expression demonstrated in Equation1 (from Medero et al. 2009)

$$CP = \frac{e_i - e_f}{1 + e_0} \qquad (1)$$

Where, e_i = equilibrium void ratio from *1D* consolidation oedometer test of as-compacted specimen, e_f = equilibrium void ratio from *1D* consolidation oedometer test of saturated specimen (inundated specimen), e_0 = initial void ratio of the specimen corresponding to the dry density of the sample, *CP* = collapse potential.

Table 1: Geotechnical and mineralogical properties of expansive soils

Soil No.	Soil Name	DFSI (%)	Q (%)	M_o (%)	K/H (%)	G (%)	Sand (%)	Silt (%)	Clay (%)	PI (%)	G_s
S1	Nagpur	134	45	55	0	0	5	28	67	55	2.77
S2	Bharuch	104	43	40	17*	0	6	35	59	34	2.74
S3	B-D highway	70	50	34	17*	0	10	30	60	40.3	2.72
S4	Ahmedabad	30	86	12	2#	1	15	52	32	31	2.70

*Halloysite, # Kaolinite, *G*-Gravel

Table 2: Swelling, matric suction and collapse potential response of unsaturated expansive soils

Soil Name	**Soil Name**	***DFSI* (%)**	**S_r (%)**	**P_S (kPa)**	**u_a-u_w (kPa)**	***CP* (%) @400kPa**	***CP* (%) @800kPa**
S1	Nagpur	134	30	90	34386	9.23	13.56
			43	76	13348	7.12	12.59
			52	71	12460	6.27	9.21
			62	59	3653	4.6	6.67
			75	43	2654	0.27	1.91
S2	Bharuch	104	30	68	21000	9.17	12.87
			43	57	10436	6.57	9.17
			53	36	6852	5.31	6.67
			66	33	3990	3.80	5.75
			75	29	3580	3.54	5.63
			84	17	1560	2.45	5.60
			97	6	340	0.78	4.6
S3	B-D Highway Soil	70	30	65	13733	9.17	12.6
			43	51	5941	2.70	7.90
			52	28	4288	2.49	6.53
			62	25	1748	-1.49	1.49
			75	10	732	0.15	0.32
S4	Ahmedabad	30	30	13	7781	6.59	7.07
			43	10	5442	4.29	4.09
			52	8	4101	3.18	3.91
			62	5	618	0.93	1.03
			75	4	124	0.16	0.42

4. Results and Discussions

The research focuses on the evaluation of matric suction, swelling and collapsible characteristics of expansive soils along with their *DFSI* and mineralogical composition.

4.1 Influence of DFSI on matric suction characteristics of expansive soil

Matric suction in a soil develops as a result of adhesive and cohesive forces associated with the soil particle assembly (soil matrix). It could also be defined as force attracting the soil water to the soil matrix. Particle size within the soil mass would govern these phenomena. Relationship of matric suction and degree of saturation of expansive soils with varying *DFSI* are shown in the Fig 5. It could be identified that Matric suction was found to decrease with increase in the degree of saturation for all the expansive soils. It could be observed that the matric suction for the present study followed corresponding pattern S1>S2>S3>S4; as represented in Table 2. The results were analogous for all values of degree of saturation. Matric suction of the soil reduced with decrease in *DFSI* of the soil. About 4.42 times reduction in the matric suction values were observed for the lowest degree of saturation (S_r = 30%) between Nagpur soil (Highest *DFSI*) and Ahmedabad soil (Lowest *DFSI*), as shown in Table 2. Matric suction of soil S4 was found to be 21.4 times lesser as compared to that of soil S1 for 75% degree of saturation. Matric suction was found to be the function of particle size (Fredlund and Rahardjo 1993; Likos and Lu (2004). Smaller the particle size, larger is the matric suction of soil. Higher DFSI values, higher clay content, lower shrinkage limit and higher Montmorillonite content indicated that Nagpur soil (S1) contained larger amount of smaller size particles leading to higher matric suction. However, Ahmedabad soil possessing lesser *DFSI* (30%) comprised of lower amount of smaller size particles and hence resulted into lower matric suction.

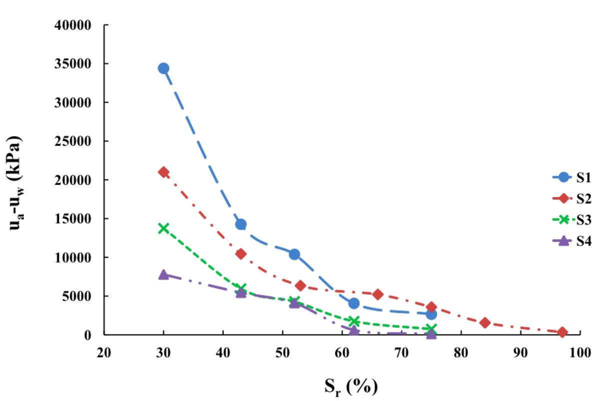

Fig 5. Variation of matric suction of expansive soils with degree of saturation.

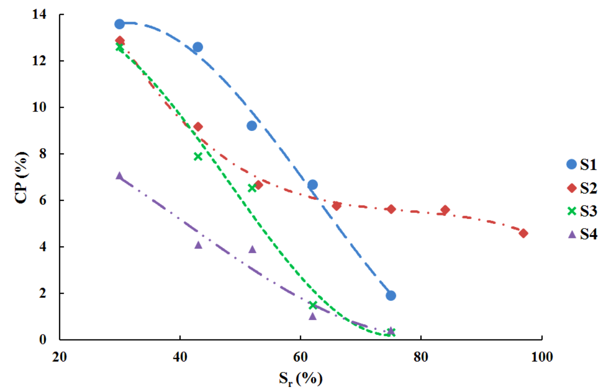

Fig 8. Collapse potential variation with degree of saturation for soils S1, S2, S3 and S4.

4.2 Influence of DFSI on swelling characteristics of expansive soils

Differential free swell index (*DFSI*) denotes the swelling prospective for a soil. Swelling pressure indicates the quantitative amount of pressure exerted by the expansive soil under saturated conditions, when volume change of soil mass is restricted. Increment in the swelling pressure with time has been displayed for soils S1, S2, S3 and S4 in Fig 6 (a), (b), (c) & (d) respectively. Trend of swelling pressure enhancement with time was found to be similar for all four soils. Swelling characteristics of all four expansive soils with respect to degree of saturation has been shown in Fig 7. A linear variation of swelling pressure (P_S) with degree of saturation (S_r) was attained for all four expansive soils (S1, S2, S3 and S4). Swelling pressure was observed to decrease with increment in the degree of saturation for all four soils (Table 2). Swelling pressure obtained from constant volume method was observed to be the maximum for S1 soil and minimum for S4 soil. Increase in the degree of saturation might lead to gradual fulfillment of affinity of water in the expansive soils yielding to lower values of suction. Montmorillonite appeared as the dominant clay mineral in S1, S2 and S3 soils (Table 1). Presence of higher clay content denoted larger negative charge due to presence of higher Montmorillonite content. Hence, the soil possessing higher clay content would require more cations to balance the negative charge for an equilibrium state (Mitchell and Soga, 2005), which would possess higher affinity for water. Therefore, the Nagpur soil contained higher capability to swell at all degree of saturation values as compared to Bharuch and B-D highway soil. Dominant mineral in Ahmedabad soil was obtained to be Quartz resulting in lowest affinity for water leading to smaller values of swell pressure for S4 soil.

4.3 Influence of DFSI on collapsible characteristics of expansive soil

Collapse potential of soil designated the degree of soil skeleton crumbling due to gradual increment in the vertical load or due to sudden upsurge of water content within the soil mass. It specified the magnitude of volume deterioration experienced by the soil specimen. Collapse potential variation in all expansive soils with their degree of saturation values at vertical stress of 800kPa are shown in Fig 8. It could be examined that the collapse potential significantly reduced with the increase in saturation values of the soil at 800kPa vertical stress. It was also identified that maximum

collapse potential was obtained for the Nagpur soil (S1) at 800kPa vertical stress (Table 2). On the contrary, lowest collapse potential was determined for Ahmedabad soil.
Soil in unsaturated state would be tightly held by the additional interparticle resistive force due to presence of air-water interface /contractile skin in unsaturated state (Pandya and Sachan, 2017b). Presence of greater amount of smaller size particles and higher percentage of Montmorillonite gave rise to the higher intensified additional inter-particle resistive force. Inter-particle resistive force would be directly proportional to matric suction, which would inversely vary with particle size. As degree of saturation increased the particles which were held tightly by intensified resistive force might lead to sudden and higher magnitude of volume change for Nagpur soil. However, as the magnitude of inter-particle resistive force decreased with the reduction in amount of clay particles (smaller size particles), the collapse potential of soil was found to reduce (Table 2).

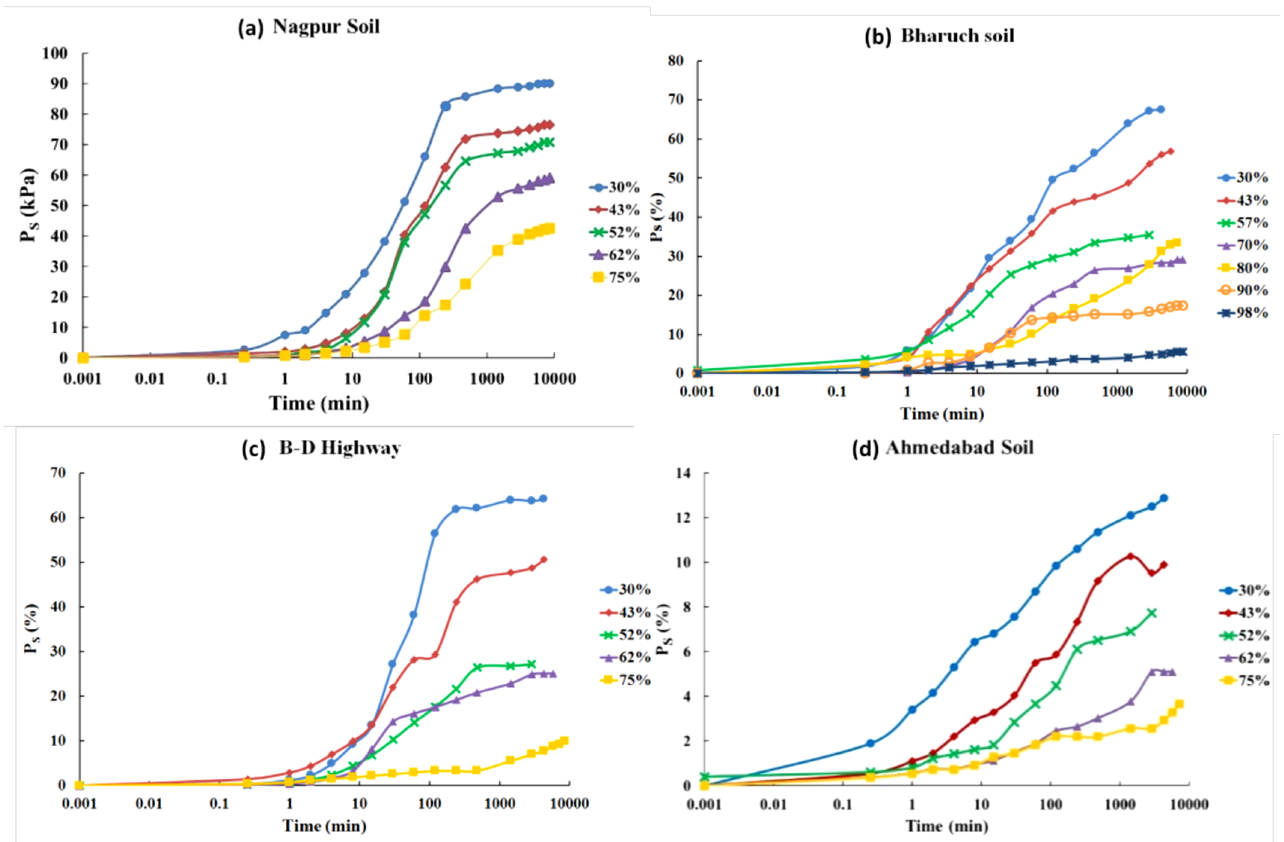

Fig 6. Transient variation of swelling pressure of expansive soils at different degree of saturation. (a) Nagpur soil, (b) Bharuch Soil, (c) Bharuch-Dahej Highway soil, (d) Ahmedabad soil

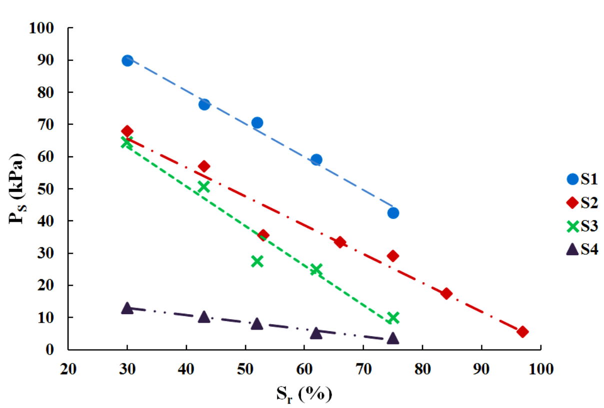

Fig 7. Variation of maximum swelling pressures of expansive soils with degree of saturation

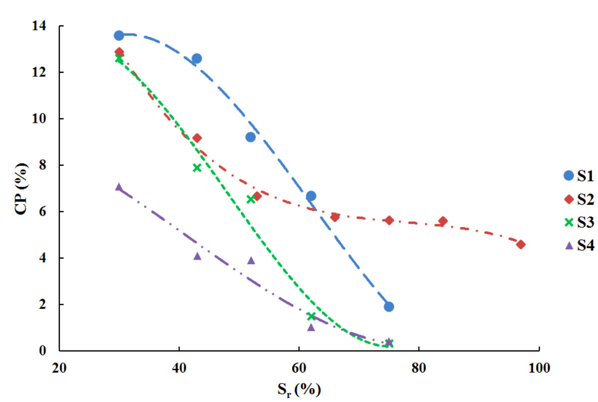

Fig 8. Collapse potential variation with degree of saturation for soils S1, S2, S3 and S4

4.4 Relationship of matric suction with swelling pressure of expansive soils

Matric suction of soil could be expressed in the form of pressure, at which the unsaturated soil would attract the water from the positive hydraulic datum (water table). Variation of matric suction with the swelling pressure of expansive soils with different *DFSI* at varying degree of saturation is shown in Fig 9. It could be attributed from the results that specimens with higher matric suction exhibited larger swelling pressure. Existence of matric suction due to presence of air-water interface gave rise to the capillary force (Pandya and Sachan, 2017b). Soil possessing large amount of Montmorillonite clay content revealed the presence of larger quantity of small size clay particles. For platy particles, Laplace equation relating matric suction of the soil to the surface tension and spherical radii (r_1 and r_2) could be reduced to the following form represented in Equation 2 (Cho and Santamarina, 2001). Schematic sketch representing the meniscus (air-water interface), spherical radii (r_1 and r_2) and distance between two platy particles are presented in Fig 10.

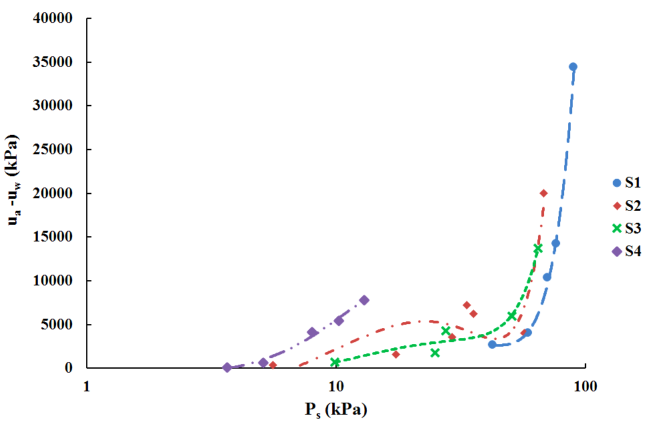

Fig 9. Relationship of swelling pressure with matric suction of expansive soils

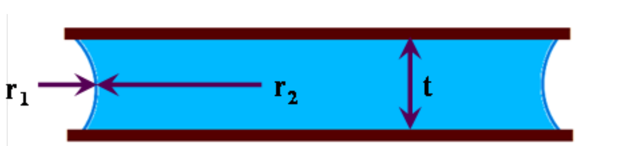

Fig 10. Schematic representation of meniscus, spherical radii (r_1 and r_2) and distance between platy clay particles (t)

$$\Delta u = T_S\left(\frac{1}{r_1}\right) \tag{2}$$

For platy particles $r_1 << r_2$, the term $(1/r_2)$ remained negligible; thus it can be neglected. The distance (t) between two platy clay particles can also be described as $t = 2*r_1$. Water content in the space between two platy particles can be described in Equation 3 (Cho and Santamarina, 2001).

$$\Delta u = \frac{W_w}{W_s} = \frac{A(2r_1)\gamma_w}{W_s} = \left(\frac{2A}{W_s/g}\right)r_1\frac{\gamma_w}{g} = \frac{S_S r_1 \gamma_w}{g}$$
……………… (3)

Where, A = surface area of one platy particle, W_s and W_w = solids and water weights, Ts = surface tension, S_S indicates specific surface area, γ_w = unit weight of water, w = water content and g = acceleration due to gravity. This formulation indicated that the matric suction between two platy particles is a function of specific surface area of soil, as shown in the Equation 4 (Cho and Santamarina, 2001).

$$\Delta u = T_S\left(\frac{S_S \gamma_w}{wg}\right) \tag{4}$$

Soils consisting of larger amount of clay particles acquired higher specific surface area; hence this might have proceeded to the development of high matric suction within the soil mass. This would have resulted in the development of intensified additional inter-particle resistive force due to larger matric suction as represented in Equation 5 (Likos and Lu, 2004).

$$F_e = (u_a - u_w)\pi r_2^{\,2} + T_s 2\pi r_2 \tag{5}$$

This might lead to the intense attraction between two platy particles together which would cause reduced interlayer spacing between two individual Montmorillonite structural units (Tan and Kong, 2001). Hence, this would have contributed to development of higher overall unbalanced negative charge on the surface of clay particle, which would result in higher affinity for water to reach equilibrium. This would foster higher crystalline swelling among two structural units, which would lead to higher swelling pressure in the soil possessing high matric suction with large *DFSI*.

4.5 Relationship of matric suction with Collapse Potential of expansive soils

Collapse of the soil skeleton occurs due to removal of the cementing agents bonding the soil particles together within soil mass due to upsurge in quantity of water in soil specimen or due to rise in the overburden (vertical stress). Transient variation in the environmental and climatic conditions could exhibit changes in matric suction of the soil mass which would instigate alterations inside the soil fabric arrangement. Variation of collapse potential with matric suction of the soil has been evaluated and signified in Fig 11. Polynomial variation of collapse potential with matric suction was observed for all expansive soils (S1, S2, S3 and S4). The schematic diagram to understand the collapse mechanism of unsaturated soil skeleton on saturation and vertical stress augmentation has been shown in Fig 12 (a) & (b) respectively. It could be acclaimed from the quantitative estimation of collapsible and matric suction characteristics of the expansive soils (S1, S2, S3 and S4) that collapse potential of the soil was found to be maximum for the soil possessing more matric suction (Table 2). Collapse potential decreased with reduction in the matric suction of soil irrespective of the degree of saturation.

Soil possessing higher matric suction contributed to the development of higher capillary pressure causing intensified hold amongst soil particles. Nagpur soil underwent extreme volumetric deformation due to sudden inundation and vertical stress augmentation. When soil specimen with high capillary pressure was subjected to larger vertical stress and sudden saturation, it would cause greater magnitude/amount of localized deformation due to sudden disappearance of air-water interface leading to weakening of additional inter-particle resistive force within the soil skeleton causing enormous collapse. However, smaller matric suction would create lower capillary force, which would cause lower magnitude of collapse due to little change in volumetric arrangement within the soil mass.

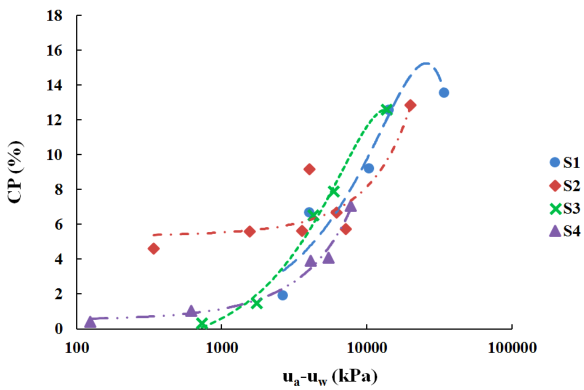

Fig 11. Relationship of collapse potential of expansive soils with matric suction

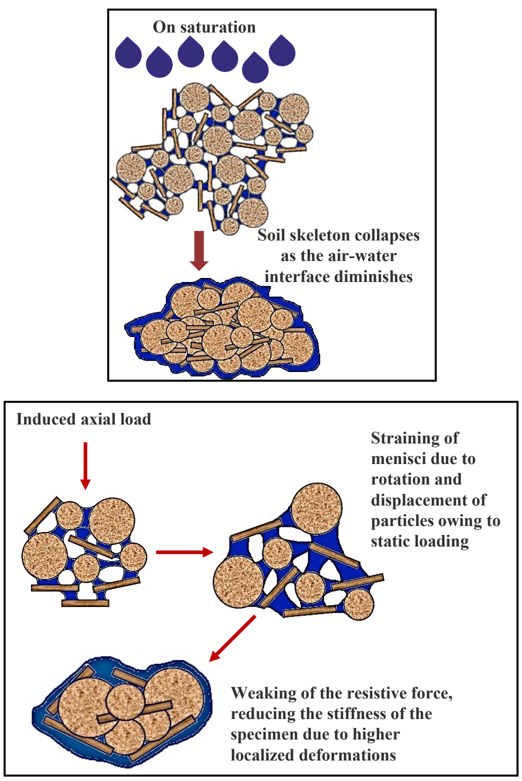

Fig 12. Conceptual sketch representing collapse mechanism within soil skeleton, (a) On saturation, (b) On vertical stress augmentation

5. Conclusions

Extensive experimental research was performed to evaluate the swelling, collapsible and matric suction characteristics of four different expansive soils with different mineralogical composition and *DFSI*. These soil samples were collected from Nagpur, Bharuch, Bharuch-Dahej Highway and Ahmedabad soil. Main observations drawn from the study are as follows:

1. Matric suction was obtained to be the maximum for soils with largest *DFSI* regardless of their degree of saturation. At lowest degree of saturation, the matric suction of Nagpur expansive soil was attained to be 4.42 times higher as compared to Ahmedabad soil.
2. The linear relationship of swelling pressure with degree of saturation was obtained for expansive soils with *DFSI* varying from 30% to 134%. Minimum swell pressure was obtained for the expansive soil with lowest *DFSI*. Nagpur expansive soil exhibited highest percentage of Montmorillonite and the maximum matric suction. This revealed larger swelling pressures due to large amount of crystalline swelling owing to the development of intense capillary pressure within soil mass.
3. Larger magnitude of volumetric deformation due to the collapse of soil skeleton was observed for soil with higher *DFSI*, higher matric suction and larger amount of Montmorillonite. Largest collapse potential (14%) was obtained for Nagpur soil specimen prepared at lowest degree of saturation, which was obtained to be two times higher than Ahmedabad soil specimen at same degree of saturation.

The results and findings from the current study signifying the swelling and collapsible characteristics of four expansive soils could be applicable for any expansive soils possessing equivalent grain size distribution and *DFSI* values.

Acknowledgements

Financial Support from IIT Gandhinagar is gratefully acknowledged. Any opinions, findings, and conclusions or recommendations expressed in this material are those of authors and do not necessarily reflect the views of IIT Gandhinagar.

References

ASTM D5298-10 (2013). Standard test method for measurement of soil potential (suction) using filter paper. *D5298-10, West Conshohocken, Pennsylvania, USA*.

Charlie, W. A., Osman, M. A., and Ali, E. M. (1984). Construction on expansive soils in Sudan. *Journal of Construction Engineering and Management*, 110(3), 359-374.

Cho, G. C., & Santamarina, J. C. (2001). Unsaturated particulate materials-particle-level studies. *Journal of geotechnical and geoenvironmental engineering*, 127(1), 84-96.

Fredlund, D. G., and Rahardjo, H. (1993). Soil mechanics for unsaturated soils, *John Wiley & Sons*.

Houston, S. L., Dye, H. B., Zapata, C. E., Walsh, K. D., and Houston, W. N. (2009). Study of expansive soils and residential foundations on expansive soils in Arizona. *Journal of performance of constructed facilities*, 25 (1), 31-44.

Likos, W. J., & Lu, N. (2004). Hysteresis of capillary stress in unsaturated granular soil. *Journal of Engineering mechanics*, 130(6), 646-655.

Medero, G. M., Schnaid, F., & Gehling, W. Y. (2009). Oedometer behavior of an artificial cemented highly collapsible soil. *Journal of Geotechnical and Geoenvironmental Engineering*, 135(6), 840-843.

Mitchell, J. K., & Soga, K. (2005). Fundamentals of soil behavior, *John Wiley & Sons*.

Nalbantoglu, Z., & Gucbilmez, E. (2001). Improvement of calcareous expansive soils in semi-arid environments. *Journal of arid environments*, 47(4), 453-463.

Nelson, J., and Miller, D. J. (1997). Expansive soils: problems and practice in foundation and pavement engineering. *John Wiley and Sons*.

Nowamooz, H., & Masrouri, F. (2010). Suction variations and soil fabric of swelling compacted soils. *Journal of Rock Mechanics and Geotechnical Engineering*, 2(2), 129-134.

Pandya, S. and Sachan, A. (2017a). Effect of matric suction and initial static loading on dynamic behavior of unsaturated cohesive soil. *International Journal of Geotechnical Engineering*, Taylor & Francis, online available, 23 Feb 2017.

Pandya, S. and Sachan, A. (2017b). Variation of collapse potential and stiffness degradation with matric suction of compacted unsaturated cohesive soil. *International Journal of Geotechnical Engineering*, Taylor & Francis, online available, 07 Nov 2017.

Tan, L. and Kong, L. (2001). Study of swelling-shrinkage regularity of montmorillonite crystal and its relation with matric suction, Science in China Series D-Earth Sciences, 44(6), 498-507.

Verma, S. K., & Maru, S. (2013). Behaviourial study of expansive soils and its effect on structures–A review. *International Journal of Innovations in Engineering and Technology*, 2(2), 228-238.

Notation

u_a-u_w	= Matric suction
1D	= One dimensional
CP	= Collapse potential
CH	= Cohesive soil with high ccompressibility
e_0	= Initial void ratio of the specimen
e_i	= Initial void ratio
e_f	= Equilibrium void ratio of saturated specimen
S_r	= Degree of saturation
w	= Water content
LL	= Liquid limit
PL	= Plastic limit
SL	= Shrinkage limit
d	= Diameter
h	= Height
DFSI	= Differential free swell index
P_s	= Swell Pressure
ρ_{di}	= Initial dry density
w_i	= Initial water content
u_w	= Pore water pressure
R	= Radius of curvature
T_S	= Surface tension
α	= Contact angle
θ	= Wetting angle
p	= Vapour pressure
p_0	= Saturation vapour pressure
T	= Temperature
M	= Molecular mass
Q	= Quartz
K	= Kaolinite
H	= Halloysite
M_o	= Montmorillonite
G	= Gravel

Journal of Geotechnical and Transportation Engineering
Volume 4 | Issue 1
First Principles Derivation of Differential Equations of Equilibrium of Anisotropic Rectangular Thin Plates...
Ike
Received 5/12/2018 Accepted 6/1/2018
Published 7/1/2018
Corresponding Author:
Charles Chinwuba Ike;
charlesike@esut.edu.ng
www.jgtte.com

First Principles Derivation of Differential Equations of Equilibrium of Anisotropic Rectangular Thin Plates on Elastic Foundations

Charles Chinwuba Ike
Department of Civil Engineering, Enugu State University of Science & Technology, Enugu State, Nigeria.
Email: ikecc2007@yahoo.com, charlesike@esut.edu.ng

Abstract

In this paper, the partial differential equations of equilibrium for thin rectangular anisotropic plates resting on elastic foundations are derived from fundamental principles of the theory of elasticity. The derivations were done by simultaneous first principles consideration of the requirements of kinematic relations, material constitutive relations, and the differential equations of static equilibrium. The derivation considered transverse distributed load on the plate domain, and inplane loads. Orthotropic plate on elastic foundation equations and isotropic plate on elastic foundation equations were obtained as special cases of anisotropic plates on elastic foundations.

Keywords: *Anisotropic plate, orthotropic plate, isotropic plate, elastic foundation.*

1. Introduction

The interaction between structures and supporting soil media is of fundamental importance in foundation analysis and design and has attracted the attention of researchers [1]. The structures are modeled as beams and/or plates, and the soil media as elastic foundations. The structure soil interaction problem reduces to the analysis of beams and plates resting on elastic foundations, and such problems find important applications in the design and analysis of foundations such as individual footings, combined footings and mat (raft) foundations.

Plates are classified as thin plates with small deflection, moderately thick plates and thick plates. Thin plate theories are due to Kirchhoff, Love, Lagrange and Germain. Theories for moderately thick plates were due to Mindlin [2], Reissner [3, 4]. The mathematical theory of elasticity is used to describe the behaviour of thick plates. Shear deformation theories of plates have also been formulated by Shimpi [5], Reddy [6].

Elastic foundation models that have been used to model the interaction of the soil medium on the structure are: discrete foundation parameter models and elastic continuum models. The elastic continuum models idealise the soil medium as an elastic half space, and use the solutions of the classical theory of elasticity for half space regions [7, 8]. The classical Boussinesq problem is used to obtain analytical expressions for the reactive pressure of the soil medium on the structure.

Discrete parameter models are based on replacing the soil medium with a set of discrete elastic springs, where each spring is connected to one another with shear coupling links, in order to stimulate the continuity of the discrete model. The simplest discrete foundation model was formulated by Winkler [9] who assumed the foundation is replaced with discrete independent linear elastic springs that are closely spaced as shown in Figure 1. In the Winkler model, the soil reaction pressure at any point on the plate is directly proportional to the deflection of the plate at the point, and the proportionality constant, k, is called the modulus of subgrade reaction or the Winkler foundation parameter or modulus. The mathematical equation for the Winkler model is:

$$p_s(x, y) = kw(x, y) \qquad (1)$$

Despite the obvious advantage of simplicity in mathematical terms, the disadvantage of the Winkler model include:

(i) the foundation does not deform beyond the loaded region and this contravenes practical reality.
(ii) the Winkler model suffers from a lack of continuity in the supporting soil medium.
(iii) there is difficulty in determining the stiffness of the elastic springs to characterize the soil medium.

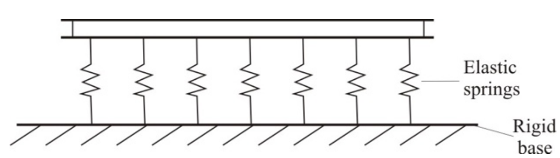

Figure 1: Winkler foundation model

Other discrete foundation models include Filonenko-Borodich foundation model, Pasternak [10] foundation model, generalised two parameter foundation model, Hetenyi [11] foundation model, and Kerr foundation model. In the Filonenko-Borodich [12] foundation, the interaction and continuity between the discrete individual spring elements is introduced by connecting the top of the spring to a thin stretched elastic membrane which is under a constant tensile force, T as shown in Figure 2.

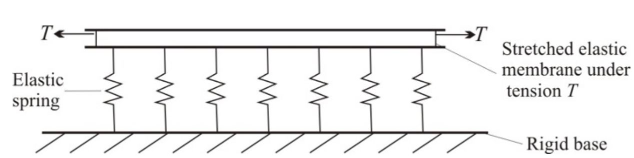

Figure 2: Filonenko-Borodich foundation model

The soil reaction pressure, $p(x, y)$ of interaction with the foundation for this model is expressed mathematically as:

$$p_s(x, y) = kw(x, y) - T\nabla^2 w(x, y) \tag{2}$$

where k and T are the two parameters of the Filonenko-Borodich model and

$$\nabla^2 = \frac{\partial^2}{\partial x^2} + \frac{\partial^2}{\partial y^2} \tag{3}$$

∇^2 is the Laplace operator.

The intensity of the tensile force T in the stretched elastic membrane characterizes the interaction of the discrete spring elements. In the Pasternak [10] foundation model, the interaction of the discrete spring elements is introduced by connecting their ends to a plate that undergoes only transverse shear deformation as shown in Figure 3. The soil pressure of interaction on the structure is given mathematically as

$$p_s(x, y) = kw(x, y) - G\nabla^2 w(x, y) \tag{4}$$

where G is the shear modulus of the shear layer, and k and G are the two discrete foundation parameters of the Pasternak foundation.

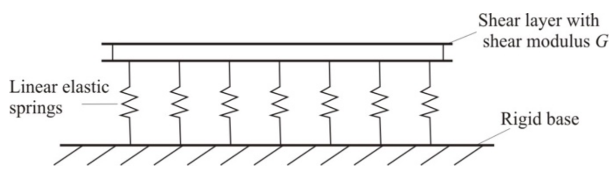

Figure 3: Pasternak foundation model

The continuity in the Pasternak foundation is characterized by the shear modulus G. Hetenyi's foundation introduces inter-spring element continuity by incorporation of an elastic plate capable of flexural deformation at the top of the springs as shown in Figure 4.

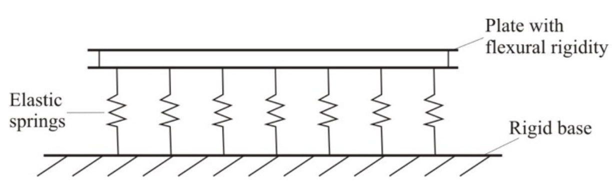

Figure 4: Hetenyi Foundation model

The model equation is:

$$p_s(x, y) = kw(x, y) - D\nabla^2\nabla^2 w(x, y) \tag{5}$$

$$p_s(x, y) = kw(x, y) - D\nabla^4 w(x, y) \tag{6}$$

where $$\nabla^4 = \nabla^2\nabla^2 = \frac{\partial^4}{\partial x^4} + 2\frac{\partial^4}{\partial x^2 \partial y^2} + \frac{\partial^4}{\partial y^4} \tag{7}$$

∇^4 is the biharmonic operator, and D is the flexural rigidity of the elastic plate.

In the Kerr [13, 14] model, the soil medium is replaced by a set of discrete elastic springs separated by a shear layer with shear modulus G, with the spring constants in the first and second layers having different values as shown in Figure 5.

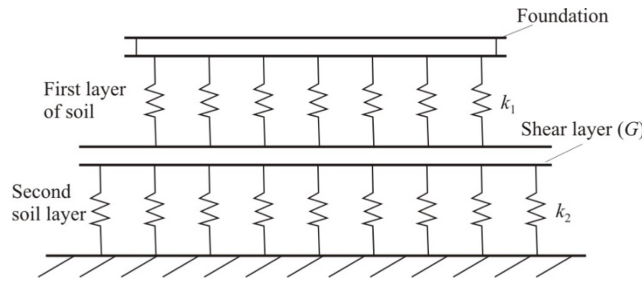

Figure 5: Kerr foundation model

The Kerr foundation model equation is given by:

$$\left(1 + \frac{k_2}{k_1}\right)p_s = \frac{G}{k_1}\nabla^2 p_s + k_2 w - G\nabla^2 w \tag{8}$$

where k_1 is the elastic spring constant for the first soil layer, k_2 is the elastic spring constant for the second soil layer and $w(x, y)$ is the deflection.

1.1 Applications of the plate on elastic foundation problem

Plate on elastic foundation problems have extensive applications in the design of highway and airport runway pavements and machine foundations. Many partial differential equations in engineering are of the same form as the plate on elastic foundation equation, and hence are analogues of the plate on elastic foundation problem. The governing equations of plate strips subjected to transverse line loads are analogous to the equation of plate on elastic foundation.

The research aim is to derive the differential equation of equilibrium of thin rectangular anisotropic plates resting on elastic foundations. The objectives include:

(i) to determine the internal stress resultants in anisotropic thin rectangular plates resting on elastic foundations.

(ii) to obtain partial differential equations of equilibrium of anisotropic thin rectangular plates on elastic foundations for the general case of transverse distributed load and inplane loads.

(iii) to obtain partial differential equations of equilibrium for special types of anisotropic plates on elastic foundation called orthotropic plates on elastic foundations and isotropic plates on elastic foundations.

2. Theoretical Framework and Methodology

2.1 Basic assumptions

This work is based on the following assumptions of the small deformation, thin plate theory:

(i) the plate material is linear elastic, homogeneous and anisotropic

(ii) the plate surface is initially flat before the application of load
(iii) the transverse deflection of the middle surface is small compared with the plate thickness
(iv) the straight lines initially normal to the middle surface of the plate before bending remain straight and normal to the middle surface during deformation, and are unchanged in length. This assumption called the normality condition, implies that the shear strains in the transverse direction (γ_{xz} and γ_{yz}) are negligible, and the normal strain ε_{zz} in the transverse direction is also negligible
(v) the stress normal to the middle plane σ_{zz} is small as compared with the other stress components, and can be disregarded without introducing significant errors.
(vi) the middle plane is free of strains, and is neutral during bending.

2.2 Equations of elasticity theory

This work applies the equilibrium approach in the theory of elasticity. Hence the equations are built on a simultaneous consideration of the three requirements of (i) kinematic relations, (ii) material constitutive laws, and (iii) differential equations of equilibrium.
For small deformation assumptions, the kinematic relations are:

$$\varepsilon_{xx} = \frac{\partial u}{\partial x} \tag{9}$$

$$\varepsilon_{xx} = \frac{\partial v}{\partial y} \tag{10}$$

$$\varepsilon_{zz} = \frac{\partial w}{\partial z} \tag{11}$$

$$\gamma_{xy} = \frac{\partial u}{\partial y} + \frac{\partial v}{\partial x} \tag{12}$$

$$\gamma_{xz} = \frac{\partial w}{\partial x} + \frac{\partial u}{\partial z} \tag{13}$$

$$\gamma_{yz} = \frac{\partial w}{\partial y} + \frac{\partial v}{\partial z} \tag{14}$$

where u, v, w are the displacement components in the x, y, and z Cartesian coordinate directions, respectively, $\varepsilon_{xx}, \varepsilon_{yy}, \varepsilon_{zz}$ are the normal strains in the x, y, and z coordinate directions γ_{xy}, γ_{yz} and γ_{xz} are the shear strains.
The material constitutive relations for anisotropic plate materials is given in matrix form by:

$$\begin{pmatrix} \varepsilon_{xx} \\ \varepsilon_{yy} \\ \varepsilon_{zz} \\ \gamma_{yz} \\ \gamma_{zx} \\ \gamma_{xy} \end{pmatrix} = \begin{pmatrix} a_{11} & a_{12} & \cdots & a_{16} \\ a_{21} & a_{22} & \cdots & a_{26} \\ & & & \\ & & & \\ & & & \\ a_{61} & a_{62} & & a_{66} \end{pmatrix} \begin{pmatrix} \sigma_{xx} \\ \sigma_{yy} \\ \sigma_{zz} \\ \tau_{yz} \\ \tau_{zx} \\ \tau_{xy} \end{pmatrix} \tag{15}$$

where $\sigma_{xx}, \sigma_{yy}, \sigma_{zz}$ are the normal stresses in the x, y, and z directions, τ_{xy}, τ_{yz}, and τ_{zx} are the shear stresses and a_{ij}, $i = 1, \ldots, 6$, $j = 1, \ldots, 6$ are the elastic constants.

The differential equations of equilibrium (static equilibrium) of an infinitesimal part of the plate element is given by the system of equations:

$$\frac{\partial \sigma_{xx}}{\partial x} + \frac{\partial \tau_{yx}}{\partial y} + \frac{\partial \tau_{zx}}{\partial z} + f_x = 0 \tag{16}$$

$$\frac{\partial \tau_{xy}}{\partial x} + \frac{\partial \sigma_{yy}}{\partial y} + \frac{\partial \tau_{zy}}{\partial z} + f_y = 0 \tag{17}$$

$$\frac{\partial \tau_{xz}}{\partial x} + \frac{\partial \tau_{yz}}{\partial y} + \frac{\partial \sigma_{zz}}{\partial z} + f_z = 0 \tag{18}$$

where f_x, f_y and f_z are the body force components on the x, y and z coordinate directions.

3. Derivation of Equations of Anisotropic Thin Plates on Elastic Foundations

3.1 Displacement field

The derivation proceeds on the assumption that the displacement at any point on the plate can be determined from the transverse displacement of the plate middle surface denoted by $w(x, y)$; and that the in-plane displacement components are given in terms of $w(x, y)$ by:

$$u = -z\frac{\partial w}{\partial x} \tag{19}$$

$$v = -z\frac{\partial w}{\partial y} \tag{20}$$

where z is the distance from the middle plane.

3.2 Strain field

Applying Equations (19) and (20) in the kinematic relations, and using the foundational assumptions, the strain fields are obtained as:

$$\varepsilon_{xx} = -z\frac{\partial^2 w}{\partial x^2} \tag{21}$$

$$\varepsilon_{yy} = -z\frac{\partial^2 w}{\partial y^2} \tag{22}$$

$$\gamma_{xy} = -2z\frac{\partial^2 w}{\partial x \partial y} \tag{23}$$

$$\gamma_{xz} = 0 \tag{24}$$

$$\gamma_{yz} = 0 \tag{25}$$

3.3 Stress-strain relations

For anisotropic thin plates, the material constitutive relations given in general as Equation (15) simplify to become:

$$\begin{pmatrix} \sigma_{xx} \\ \sigma_{yy} \\ \tau_{xy} \end{pmatrix} = \begin{pmatrix} g_{11} & g_{12} & g_{16} \\ g_{12} & g_{22} & g_{26} \\ g_{16} & g_{26} & g_{66} \end{pmatrix} = \begin{pmatrix} \varepsilon_{xx} \\ \varepsilon_{yy} \\ \gamma_{xy} \end{pmatrix} \tag{26}$$

where g_{11}, g_{12}, g_{16} … g_{66} are the elastic constants.

Using Equations (21) – (23), the stress fields are obtained as:

$$\sigma_{xx} = -z\left(g_{11}\frac{\partial^2 w}{\partial x^2} + g_{12}\frac{\partial^2 w}{\partial y^2} + 2g_{16}\frac{\partial^2 w}{\partial x \partial y}\right) \quad (27)$$

$$\sigma_{yy} = -z\left(g_{12}\frac{\partial^2 w}{\partial x^2} + g_{22}\frac{\partial^2 w}{\partial y^2} + 2g_{26}\frac{\partial^2 w}{\partial x \partial y}\right) \quad (28)$$

$$\tau_{xy} = -z\left(g_{16}\frac{\partial^2 w}{\partial x^2} + g_{26}\frac{\partial^2 w}{\partial y^2} + 2g_{66}\frac{\partial^2 w}{\partial x \partial y}\right) \quad (29)$$

The shear stresses τ_{zx} and τ_{zy} are obtained using the differential equations of equilibrium Equations (16-18) as follows:

$$\frac{\partial \tau_{zx}}{\partial z} = z\left(g_{11}\frac{\partial^3 w}{\partial x^3} + 3g_{16}\frac{\partial^3 w}{\partial x^2 \partial y} + (g_{12}+2g_{66})\frac{\partial^3 w}{\partial x \partial y^2} + g_{26}\frac{\partial^3 w}{\partial y^3}\right) \quad \ldots(30)$$

$$\frac{\partial \tau_{zy}}{\partial z} = z\left(g_{16}\frac{\partial^3 w}{\partial x^3} + 3g_{26}\frac{\partial^3 w}{\partial x \partial y^2} + (g_{12}+2g_{66})\frac{\partial^3 w}{\partial x^2 \partial y} + g_{22}\frac{\partial^3 w}{\partial y^3}\right) \quad \ldots(31)$$

Integration with respect to z, where $-h/2 \leq z \leq h/2$, gives:

$$\tau_{zx} = \frac{1}{2}\left(z^2 - \frac{h^2}{4}\right)\left\{ g_{11}\frac{\partial^3 w}{\partial x^3} + 3g_{26}\frac{\partial^3 w}{\partial x^2 \partial y} + (g_{12}+2g_{66})\frac{\partial^3 w}{\partial x \partial y^2} + g_{26}\frac{\partial^3 w}{\partial y^3}\right\} \quad (32)$$

$$\tau_{zy} = \frac{1}{2}\left(z^2 - \frac{h^2}{4}\right)\left\{ g_{16}\frac{\partial^3 w}{\partial x^3} + 3g_{26}\frac{\partial^3 w}{\partial x \partial y^2} + (g_{12}+2g_{66})\frac{\partial^3 w}{\partial x^2 \partial y} + g_{22}\frac{\partial^3 w}{\partial y^3}\right\} \quad (33)$$

3.4 Stress resultants

The stress resultants are given by the bending moments M_{xx}, M_{yy}, the twisting moments M_{xy} and the shear forces Q_x, Q_y as follows:

$$M_{xx} = \int_{-h/2}^{h/2} \sigma_{xx}\, z\, dz \quad (34)$$

$$M_{yy} = \int_{-h/2}^{h/2} \sigma_{yy}\, z\, dz \quad (35)$$

$$M_{xy} = M_{yx} = \int_{-h/2}^{h/2} \tau_{xy}\, z\, dz \quad (36)$$

$$Q_x = \int_{-h/2}^{h/2} \tau_{xz}\, dz \quad (37)$$

$$Q_y = \int_{-h/2}^{h/2} \tau_{yz}\, dz \quad (38)$$

Substitution of Equations (27-29), (32) and (33) yields:

$$M_{xx} = -\int_{-h/2}^{h/2} z^2\left(g_{11}\frac{\partial^2 w}{\partial x^2} + g_{12}\frac{\partial^2 w}{\partial y^2} + 2g_{16}\frac{\partial^2 w}{\partial x \partial y}\right)dz \quad (39)$$

$$M_{yy} = -\int_{-h/2}^{h/2} z^2\left(g_{12}\frac{\partial^2 w}{\partial x^2} + g_{22}\frac{\partial^2 w}{\partial y^2} + 2g_{26}\frac{\partial^2 w}{\partial x \partial y}\right)dz \quad (40)$$

$$M_{xy} = -\int_{-h/2}^{h/2} z^2\left(g_{16}\frac{\partial^2 w}{\partial x^2} + g_{26}\frac{\partial^2 w}{\partial y^2} + 2g_{66}\frac{\partial^2 w}{\partial x \partial y}\right)dz \quad (41)$$

$$Q_x = \int_{-h/2}^{h/2} \frac{1}{2}\left(z^2 - \frac{h^2}{4}\right)dz\left(g_{11}\frac{\partial^3 w}{\partial x^3} + 3g_{16}\frac{\partial^3 w}{\partial x^2 \partial y} + (g_{12}+2g_{66})\frac{\partial^3 w}{\partial x \partial y^2} + g_{26}\frac{\partial^3 w}{\partial y^3}\right) \quad \ldots(42)$$

$$Q_y = \int_{-h/2}^{h/2} \frac{1}{2}\left(z^2 - \frac{h^2}{4}\right)dz\left(g_{16}\frac{\partial^3 w}{\partial x^3} + 3g_{26}\frac{\partial^3 w}{\partial x \partial y^2} + (g_{12}+2g_{66})\frac{\partial^3 w}{\partial x^2 \partial y} + g_{22}\frac{\partial^3 w}{\partial y^3}\right) \quad \ldots(43)$$

Evaluation of the integrals and simplification yields:

$$M_{xx} = -\left(D_{11}\frac{\partial^2 w}{\partial x^2} + D_{12}\frac{\partial^2 w}{\partial y^2} + 2D_{16}\frac{\partial^2 w}{\partial x \partial y}\right) \quad (44)$$

$$M_{yy} = -\left(D_{12}\frac{\partial^2 w}{\partial x^2} + D_{22}\frac{\partial^2 w}{\partial y^2} + 2D_{26}\frac{\partial^2 w}{\partial x \partial y}\right) \quad (45)$$

$$M_{xy} = -\left(D_{16}\frac{\partial^2 w}{\partial x^2} + D_{26}\frac{\partial^2 w}{\partial y^2} + 2D_{66}\frac{\partial^2 w}{\partial x \partial y}\right) \quad (46)$$

$$Q_x = -\left(D_{11}\frac{\partial^3 w}{\partial x^3} + 3D_{16}\frac{\partial^3 w}{\partial x^2 \partial y} + (D_{12}+2D_{66})\frac{\partial^3 w}{\partial x \partial y^2} + D_{26}\frac{\partial^3 w}{\partial y^3}\right) \quad \ldots(47)$$

$$Q_y = -\left(D_{16}\frac{\partial^3 w}{\partial x^3} + (D_{12}+2D_{66})\frac{\partial^3 w}{\partial x^2 \partial y} + 3D_{26}\frac{\partial^3 w}{\partial x \partial y^2} + D_{22}\frac{\partial^3 w}{\partial y^3}\right) \quad \ldots(48)$$

where in general,

$$\int_{-h/2}^{h/2} z^2 g_{ij}\, dz = \frac{g_{ij}h^3}{12} = D_{ij} \quad (49)$$

D_{11}, D_{12} are bending rigidities, D_{66} is the twisting rigidity, D_{16}, D_{26} are coupling rigidities or secondary rigidities.

3.5 Differential equations of equilibrium

The differential equations of equilibrium in terms of the stress resultants are:

$$\frac{\partial Q_x}{\partial x} + \frac{\partial Q_y}{\partial y} + q(x,y) - p_s(x,y) = 0 \quad (50)$$

$$\frac{\partial M_{xx}}{\partial x} + \frac{\partial M_{xy}}{\partial y} - Q_x = 0 \quad (51)$$

$$\frac{\partial M_{xy}}{\partial x} + \frac{\partial M_{yy}}{\partial y} - Q_y = 0 \quad (52)$$

Equations (50) – (52) can be expressed as the single equation:

$$\frac{\partial}{\partial x}\left(\frac{\partial M_{xx}}{\partial x} + \frac{\partial M_{xy}}{\partial y}\right) + \frac{\partial}{\partial y}\left(\frac{\partial M_{xy}}{\partial x} + \frac{\partial M_{yy}}{\partial y}\right) + q = 0 \quad (53)$$

$$\frac{\partial^2 M_{xx}}{\partial x^2} + 2\frac{\partial^2 M_{xy}}{\partial x \partial y} + \frac{\partial^2 M_{yy}}{\partial y^2} + q = 0 \quad (54)$$

Then by substitution of Equations (44-46), we obtain upon simplification,

$$D_{11}\frac{\partial^4 w}{\partial x^4}+4D_{16}\frac{\partial^4 w}{\partial x^3\partial y}+(2D_{12}+4D_{66})\frac{\partial^4 w}{\partial x^2\partial y^2}$$
$$+\ 4D_{26}\frac{\partial^4 w}{\partial x\partial y^3}+D_{22}\frac{\partial^4 w}{\partial y^4}+p_s(x,y)=q(x,y) \qquad (55)$$

Equation (55) is the governing partial differential equation of equilibrium of anisotropic rectangular thin plates on elastic foundation under distributed transverse loads $q(x, y)$. For orthotropic plates, $D_{16} = D_{26} = 0$ and the differential equation of equilibrium simplifies to become:

$$D_{11}\frac{\partial^4 w}{\partial x^4}+2(D_{12}+2D_{66})\frac{\partial^4 w}{\partial x^2\partial y^2}+D_{22}\frac{\partial^4 w}{\partial y^4}+p_s(x,y)=q(x,y)$$
…(56)

or,

$$D_{xx}\frac{\partial^4 w}{\partial x^4}+2H\frac{\partial^4 w}{\partial x^2\partial y^2}+D_{yy}\frac{\partial^4 w}{\partial y^4}+p_s(x,y)=q(x,y) \qquad (57)$$

where $H = D_{12} + 2D_{66}$ (58)
$D_{xx} = D_{11}$ (59)
$D_{yy} = D_{22}$ (60)

$$D_{xx}=\frac{h^3E_x}{12} \qquad (61)$$

$$D_{yy}=\frac{h^3E_y}{12} \qquad (62)$$

$$H = D_{xx} + 2G_{xy} \qquad (63)$$

$$D_{xy}=\frac{h^3E_{xy}}{12} \qquad (64)$$

$$G_{xy}=\frac{h^3G}{12} \qquad (65)$$

E_x, E_y, and G are the orthotropic plate moduli, D_{xx}, D_{yy}, D_{xy}, and G_{xy} are the flexural rigidities and the torsional rigidity of an orthotropic thin plate.
For orthotropic plates, the internal forces become:

$$M_{xx}=-\left(D_{11}\frac{\partial^2 w}{\partial x^2}+D_{12}\frac{\partial^2 w}{\partial y^2}\right)=-\left(D_{xx}\frac{\partial^2 w}{\partial x^2}+D_{xy}\frac{\partial^2 w}{\partial y^2}\right) \qquad (66)$$

$$M_{yy}=-\left(D_{12}\frac{\partial^2 w}{\partial x^2}+D_{22}\frac{\partial^2 w}{\partial y^2}\right)=-\left(D_{xy}\frac{\partial^2 w}{\partial x^2}+D_{yy}\frac{\partial^2 w}{\partial y^2}\right) \qquad (67)$$

$$M_{xy}=-\left(2D_{66}\frac{\partial^2 w}{\partial x\partial y}\right)=-2G_{xy}\frac{\partial^2 w}{\partial x\partial y} \qquad (68)$$

$$Q_x=-\left(D_{11}\frac{\partial^3 w}{\partial x^3}+(D_{12}+2D_{66})\frac{\partial^3 w}{\partial x\partial y^2}\right) \qquad (69)$$

$$Q_x=-\left(D_{xx}\frac{\partial^3 w}{\partial x^3}+(D_{xy}+2G_{xy})\frac{\partial^3 w}{\partial x\partial y^2}\right) \qquad (70)$$

$$Q_x=-\left(D_{xx}\frac{\partial^3 w}{\partial x^3}+H\frac{\partial^3 w}{\partial x\partial y^2}\right) \qquad (71)$$

$$Q_y=-\left((D_{12}+2G_{66})\frac{\partial^3 w}{\partial x^2\partial y}+D_{22}\frac{\partial^3 w}{\partial y^3}\right) \qquad (72)$$

$$Q_y=-\left(H\frac{\partial^3 w}{\partial x^2\partial y}+D_{22}\frac{\partial^3 w}{\partial y^3}\right) \qquad (73)$$

3.6 Combined transverse and inplane loading of anisotropic plate on elastic foundation

For vertical equilibrium in the z direction of an anisotropic thin plate element resting on an elastic foundation and under combined transverse and in-plane loading, Equation (50) changes to account for the inplane loads N_{xx}, N_{yy}, and N_{xy} as follows:

$$\frac{\partial Q_x}{\partial x}+\frac{\partial Q_y}{\partial y}+q(x,y)+N_{xx}\frac{\partial^2 w}{\partial x^2}+N_{yy}\frac{\partial^2 w}{\partial y^2}-p_s(x,y)+2N_{xy}\frac{\partial^2 w}{\partial x\partial y}=0$$
…(74)

The governing partial differential equation of equilibrium for rectangular thin anisotropic plates on elastic foundations under combined distributed transverse and inplane loads becomes:

$$D_{11}\frac{\partial^4 w}{\partial x^4}+4D_{16}\frac{\partial^4 w}{\partial x^3\partial y}+2(D_{12}+2D_{66})\frac{\partial^4 w}{\partial x^2\partial y^2}+4D_{26}\frac{\partial^4 w}{\partial x\partial y^3}+D_{22}\frac{\partial^4 w}{\partial y^4}+p_s(x,y)$$
$$=q(x,y)+N_{xx}\frac{\partial^2 w}{\partial x^2}+N_{yy}\frac{\partial^2 w}{\partial y^2}+2N_{xy}\frac{\partial^2 w}{\partial x\partial y} \qquad (75)$$

For orthotropic plates on elastic foundations under combined transverse and inplane loading, we obtain:

$$D_{11}\frac{\partial^4 w}{\partial x^4}+2H\frac{\partial^4 w}{\partial x^2\partial y^2}+D_{22}\frac{\partial^4 w}{\partial y^4}+p_s(x,y)$$
$$=q(x,y)+N_{xx}\frac{\partial^2 w}{\partial x^2}+N_{yy}\frac{\partial^2 w}{\partial y^2}+2N_{xy}\frac{\partial^2 w}{\partial x\partial y} \qquad (76)$$

3.7 Anisotropic plates on Winkler foundation

For Winkler foundations, the subgrade reaction pressure $p(x, y)$ at any point (x, y) under the plate is directly proportional to the deflection at that point $w(x, y)$, where the proportionality constant is the Winkler coefficient of subgrade modulus or the Winkler foundation parameter, k, and mathematically, substitution of the Winkler expression for the soil reaction into Equation (75) yields:

$$D_{11}\frac{\partial^4 w}{\partial x^4}+4D_{16}\frac{\partial^4 w}{\partial x^3\partial y}+2(D_{12}+2D_{66})\frac{\partial^4 w}{\partial x^2\partial y^2}+4D_{26}\frac{\partial^4 w}{\partial x\partial y^3}$$
$$+\ D_{22}\frac{\partial^4 w}{\partial y^4}+kw(x,y)=q(x,y)+N_{xx}\frac{\partial^2 w}{\partial x^2}+N_{yy}\frac{\partial^2 w}{\partial y^2}+2N_{xy}\frac{\partial^2 w}{\partial x\partial y}$$
…(77)

For orthotropic plates on Winkler foundations, substitution of the Winkler expression for the soil reaction with Equation (76) yields the governing differential equation of equilibrium as:

$$D_{11}\frac{\partial^4 w}{\partial x^4}+2H\frac{\partial^4 w}{\partial x^2\partial y^2}+D_{22}\frac{\partial^4 w}{\partial y^4}+kw(x,y)$$
$$=q(x,y)+N_{xx}\frac{\partial^2 w}{\partial x^2}+N_{yy}\frac{\partial^2 w}{\partial y^2}+2N_{xy}\frac{\partial^2 w}{\partial x\partial y} \qquad (78)$$

For isotropic thin plates on Winkler foundations, the governing differential equation of equilibrium is obtained from Equation (76) by substitution of the expression for the Winkler soil reaction, and noting that for isotropic, homogeneous thin plates, $D_{11} = D_{22} = H = D$, and we obtain:

$$D\left(\frac{\partial^4 w}{\partial x^4}+2\frac{\partial^4 w}{\partial x^2\partial y^2}+\frac{\partial^4 w}{\partial y^4}\right)+kw(x,y)$$

$$= q(x,y) + N_{xx}\frac{\partial^2 w}{\partial x^2} + N_{yy}\frac{\partial^2 w}{\partial y^2} + 2N_{xy}\frac{\partial^2 w}{\partial x \partial y} \quad (79)$$

where D is the flexural rigidity of the isotropic plate.

3.8Anisotropic plates on Pasternak foundations

The governing differential equations of equilibrium for anisotropic plates on Pasternak foundations are obtained respectively as:

$$D_{11}\frac{\partial^4 w}{\partial x^4} + 4D_{16}\frac{\partial^4 w}{\partial x^3 \partial y} + 2(D_{12} + 2D_{66})\frac{\partial^4 w}{\partial x^2 \partial y^2} + 4D_{26}\frac{\partial^4 w}{\partial x \partial y^3} + D_{22}\frac{\partial^4 w}{\partial y^4}$$
$$+ kw(x,y) - G\nabla^2 w(x,y) = q(x,y) + N_{xx}\frac{\partial^2 w}{\partial x^2} + N_{yy}\frac{\partial^2 w}{\partial y^2} + 2N_{xy}\frac{\partial^2 w}{\partial x \partial y} \quad \ldots(80)$$

for anisotropic plates on Pasternak foundations, and

$$D_{11}\frac{\partial^4 w}{\partial x^4} + 2H\frac{\partial^4 w}{\partial x^2 \partial y^2} + D_{22}\frac{\partial^4 w}{\partial y^4} + kw(x,y) - G\nabla^2 w(x,y)$$
$$= q(x,y) + N_{xx}\frac{\partial^2 w}{\partial x^2} + N_{yy}\frac{\partial^2 w}{\partial y^2} + 2N_{xy}\frac{\partial^2 w}{\partial x \partial y} \quad (81)$$

for orthotropic plates on Pasternak foundations, and

$$D\left(\frac{\partial^4 w}{\partial x^4} + 2\frac{\partial^4 w}{\partial x^2 \partial y^2} + \frac{\partial^4 w}{\partial y^4}\right) + kw(x,y) - G\nabla^2 w(x,y)$$
$$= q(x,y) + N_{xx}\frac{\partial^2 w}{\partial x^2} + N_{yy}\frac{\partial^2 w}{\partial y^2} + 2N_{xy}\frac{\partial^2 w}{\partial x \partial y} \quad (82)$$

for isotropic plates on Pasternak foundations.

3.9Anisotropic thin rectangular plate on Filonenko-Borodich foundation

The governing partial differential equations of equilibrium for anisotropic thin rectangular plates on Filonenko-Borodich foundations are obtained, respectively as follows:

$$D_{11}\frac{\partial^4 w}{\partial x^4} + 4D_{16}\frac{\partial^4 w}{\partial x^3 \partial y} + 2(D_{12} + 2D_{66})\frac{\partial^4 w}{\partial x^2 \partial y^2} + 4D_{26}\frac{\partial^4 w}{\partial x \partial y^3} + D_{22}\frac{\partial^4 w}{\partial y^4}$$
$$+ kw(x,y) - T\nabla^2 w(x,y) = q(x,y) + N_{xx}\frac{\partial^2 w}{\partial x^2} + N_{yy}\frac{\partial^2 w}{\partial y^2} + 2N_{xy}\frac{\partial^2 w}{\partial x \partial y} \quad \ldots(83)$$

and for the special case of anisotropy called orthotropy, $D_{16} = D_{26} = 0$, we obtain

$$D_{11}\frac{\partial^4 w}{\partial x^4} + 2H\frac{\partial^4 w}{\partial x^2 \partial y^2} + D_{22}\frac{\partial^4 w}{\partial y^4} + kw(x,y) - T\nabla^2 w(x,y)$$
$$= q(x,y) + N_{xx}\frac{\partial^2 w}{\partial x^2} + N_{yy}\frac{\partial^2 w}{\partial y^2} + 2N_{xy}\frac{\partial^2 w}{\partial x \partial y} \quad (84)$$

Isotropic plates are special anisotropic plates, where $D_{11} = D_{22} = H = D$, and we obtain,

$$D\left(\frac{\partial^4 w}{\partial x^4} + 2\frac{\partial^4 w}{\partial x^2 \partial y^2} + \frac{\partial^4 w}{\partial y^4}\right) + kw(x,y) - T\nabla^2 w(x,y)$$
$$= q(x,y) + N_{xx}\frac{\partial^2 w}{\partial x^2} + N_{yy}\frac{\partial^2 w}{\partial y^2} + 2N_{xy}\frac{\partial^2 w}{\partial x \partial y} \quad (85)$$

4. Discussion

In this paper, the partial differential equation of equilibrium of anisotropic thin rectangular plate on elastic foundation has been successfully derived. The derivation applied the equilibrium approach in the mathematical theory of elasticity. Small deformation assumptions of the elasticity theory were used to express the Cauchy equations relating strains to displacements as Equations (9-14). Generalised stress-strain laws for the general case of anisotropy was used as Equation (15). The differential equations of static equilibrium were also used as Equations (16-18). The displacement field used in the derivation were consistent with thin plate theory and are given by Equations (19) and (20). Internal stress resultants were obtained for the general case of anisotropic thin plates on elastic foundations as Equations (44-48). The partial differential equation of equilibrium of anisotropic thin plate on elastic foundation was obtained as Equation (55), for transverse distributed load. The equation was obtained as Equation (75) for anisotropic plate on elastic foundation under combined transverse and in-plane loads. The equilibrium equation for anisotropic thin plate on Winkler foundation was obtained as Equation (77) for combined transverse distributed load and inplane loads. The differential equation for anisotropic thin plate on Pasternak and Filonenko-Borodich foundations were obtained, respectively as Equations (80) and (83) for combined transverse distributed loads and inplane loads. It was also found that orthotropic thin plate on elastic foundation equations and isotropic thin plate on elastic foundation equations could be obtained as special cases of the anisotropic thin plate on elastic foundation equations.

4.1 Limitations of the governing equations derived

The basic methods/approaches – continuum and modeling methods are used in deriving equations of plates on elastic foundation. In the continuum approach, the soil is considered as elastic, elastoplastic, hypoplastic, non homogeneous, anisotropic and /or layered. This demands complex mathematical methods and analysis. The modeling approach is less complicated, and involves less complicated mathematical analysis. However, the determination of the foundation model parameter(s) is a huge problem.

4.2 Limitations of the classical plate theory

The study used the classical thin plate theory (CPT) to model the plate. The classical thin plate theory (Kirchhoff plate theory) disregards the transverse shear deformations of the plate, and can hence only correctly predict the flexural behaviours of thin plates having a ratio of thickness, h to width, a, of less than approximately 0.05 (i.e. $h/a < 0.05$).

5. Conclusions

The following conclusions are made:

(i) The differential equation of equilibrium of rectangular thin anisotropic plate resting on elastic foundations can be obtained using the equilibrium approach in the mathematical theory of elasticity.

(ii) Orthotropic thin plate on elastic foundation problems are special cases of anisotropic thin plate on elastic foundation problems where $D_{16} = D_{26} = 0$, and the equation for orthotropic thin plates on elastic foundations are obtained from the anisotropic thin plate on elastic foundations where $D_{16} = D_{26} = 0$.

(iii) Isotropic thin rectangular plate on elastic foundation problems are particular types of the general anisotropic thin rectangular plate on elastic foundation where $D_{16} = D_{26} = 0$, and $D_{11} = H = D_{22} = D$; and the equations are obtained from the anisotropic thin rectangular plate on elastic foundation equation.

References

[1] Wang Y.H., Tham L.G. and Cheung Y.K. (2005) Beams and plates on elastic foundation: a review, Progress in Structural Engineering and Materials Structural Analysis and CAD, Volume 7, Issue 4, Wiley, October/December 2005, pp. 174-182 DOI: 10.1002/pse.202.

[2] Mindlin, R.D. (1951) Influence of rotary inertia on flexural motion of isotropic, elastic plates. Journal of Applied Mechanics, Vol. 18, No 1, pp 31 – 38.

[3] Reissner E. (1944) On the theory of bending of elastic plates. Journal of Mathematics and Physics, Vol. 23, pp.184-191.

[4] Reissner E. (1945) The effect of shear deformation on the bending of elastic plates. Journal of Applied Mechanics, Vol. 12, pp 69-77.

[5] Shimpi R.P. (2002). Refined plate theory and its variants. AIAA Journal, Vol. 40, pp. 137-146.

[6] Reddy J.N. (1984) A refined non-linear theory of plates with transverse shear deformation. International Journal of Solids and Structures, Vol. 20 pp. 881-896, 1984.

[7] Seeng-Min K. (2004) Bending and vibration of a plate on elastic foundation subject to inplane compression and moving loads. International Journal of Solids and Structures, Vol. 41, Issue 20, October 2004, pp 5647-5661, Elsevier Ltd.

[8] Myslecki K. (2004) Approximate fundamental solutions of equilibrium for thin plates on elastic foundation. Archives of Civil and Mechanical Engineering, Vol IV, No 1, pp 31-40.

[9] Winkler E. (1867) Die Lebre vonder elastizitat und festigkei, Dominicus, Prague.

[10] Pasternak P.L. (1954) On a new method of analysis of an elastic foundation by means of two foundation constants (in Russian) Gosud Izd Lit po Stroitelstvu Arkhitekture Moscow.

[11] Hetenyi M. (1946) Beams on elastic foundation. The University of Michigan Press, Ann Arbour, Michigan.

[12] Filonenko-Borodich M.M. (1945) A very simple model of an elastic foundation capable of spreading load, Sbornik Moskovkovo Elecktro Instituta.

[13] Kerr A.D. (1964) Elastic and visco-elastic foundation models. Journal of Applied Mechanics, ASME, 1964, 25(80), pp 491-498.

[14] Kerr A.D. (1965) A study of a new foundation model. Acta Mechanica, Vol. 1, pp 135-147.

Journal of Geotechnical and Transportation Engineering
Volume 4 | Issue 1
Using of the Circular Road Simulator to Evaluate the Performance of Asphalt Mixtures Made of ...
Kuttah
Received 4/20/2018 Accepted 6/1/2018
Published 7/1/2018
Corresponding Author:
Dina K. Kuttah;
dina.kuttah@vti.se
www.jgtte.com

Using of the Circular Road Simulator to Evaluate the Performance of Asphalt Mixtures made of Industrial By-Products

Dina K. Kuttah
Swedish National Road and Transport Research Institute (VTI), Linköping, Sweden
Email: dina.kuttah@vti.se

Abstract

It is well known that the use of by-products (recycled), instead of natural materials help toward more environmentally friendly roads by easing landfill pressures and reducing demand of extraction. Correspondingly, this paper deals with evaluating the mechanical performance of new developed hot mix asphalt (HMA) mixtures made of alternative materials (up to 98% industrial waste materials). The paper sheds light on the long-term performance of the new developed mixtures using the accelerated load testing facilities available at VTI (the Swedish National Road and Transport Research Institute). The materials, methods and results given in this article are part of ALTERPAVE European -project findings. In this project, different types of industrial by-products, namely, reclaimed asphalt pavement (RAP), foundry sand and steel slag) have been used in different fractions to find the composition of the best asphalt mixtures made mainly of industrial wastes that can substitute the asphalt mixtures made of natural aggregates. Using the circular road simulator (CRS), twenty- eight asphalt slabs were prepared using natural and industrial by-products and tested under different testing conditions. The CRS test has been used to assess the surface deterioration, wear and the changes in macrotextures of the tested asphalt slabs under wheel loading in dry or wet conditions and under different testing temperatures to simulate summer and winter seasons. In addition, studless and studded tires have been used to traffic the asphalt slabs during the CRS testing to simulate the current roads conditions in different European countries. The test results demonstrated that by controlling the homogeneity of recycled material and by using rejuvenators of suitable quality and quantity, it is possible to obtain paving mixtures with high content of recycled materials that can satisfactory substitute the conventional asphalt mixtures made of natural materials.

Keywords: Accelerated load testing; Foundry sand; Hot mix asphalt; Reclaimed asphalt pavement; Steel slag.

1. Introduction

It is well known that the construction and maintenance of European roads consume large amounts of quarried aggregates. Based on European Aggregates Association annual review [1], the European aggregates industry covers a demand of 2.7 billion tonnes of aggregates produced every year. About 10% of the produced aggregates from the European aggregates industry goes to asphalt products. According to European Aggregates Association annual review 2017, every new 1 km of roadway requires up to 30,000 tonnes of aggregates. The use of by-products (recycled), instead of primary (natural), materials help easing landfill pressures and reducing demand of extraction. In spite of the fact that one of the major challenges of pavement engineering world-wide is to meet the ever-increasing demand of economic and physical resources related to construction by means of environmentally sustainable technologies, concerns over inferior road performance have hindered the widespread use of secondary aggregates in such applications. This is especially the case in surface layers of asphalt pavements that may represent a value application for recycled solid waste materials [2]. In such a context, several studies have been focused on using different types of road paving technologies based on the use of asphalt mixtures containing recycled materials. A variety of recyclable materials in asphalt mixtures have been used and studied such as rubber from end-of-life tires [3, 4,5 and 6], reclaimed asphalt pavement [7, 8, 9, 10 and 11], waste glass [12], steel slag [13, 14 and 15], plastic [16 and 17], by-product gypsum [18 and 19], asphalt roofing shingles [20, 21, 22 and 23] and others.

The shortage in natural aggregate is not the only problem which was behind the increase in the cost of asphalt mixtures, but the shortage and high costs of asphalt and polymers have encouraged the engineers to utilize alternative bio-oils (derived from bio-based raw materials) to be used as alternative oils in hot mix asphalt manufacturing [24].

In fact, field studies have indicated that asphalt mixtures made of alternative aggregate and bio binders should be studied further in terms of long-term performance to evaluate their suitability to substitute conventional asphalt materials [25 and 26].

Correspondingly, this paper deals with evaluating the mechanical performance of new developed hot mix asphalt (HMA) mixtures made of alternative materials (up to 98% industrial waste materials) using the VTI's circular road simulator. The materials, methods and results given in this article are part of ALTERPAVE European -project findings. After characterizing all the natural and the recycled materials to be used in manufacturing ALTERPAVE asphalt mixtures, the aggregate and asphalt binder compositions of different suggested hot mix asphalt (HMA) mixtures have been developed in asphalt laboratory at University of Cantabria (UC).

Particularly, this paper focuses on the findings gathered from an accelerated circular road simulator test. The asphalt mixtures previously validated at lab scale (at University of Cantabria) have been tested using the VTI's circular road simulator to determine the surface pavement deformations, wear and texture depending on the different existing climate conditions (wet/dry environments, high medium or low temperatures, etc.) and on the possible use of studded winter tires.

2. Material characterization

The types and properties of the materials used to prepare the asphalt mixtures for the CRS tests are presented in the following paragraphs;

2. 1. Asphalt binder

A conventional Swedish 50/70 binder and polymer modified binder PMB 45/80 – 65 have been used to prepare asphalt specimens for CRS test at VTI. The properties of the conventional binder and the polymer modified binder used in preparing the asphalt mixtures for the CRS test are illustrated in Tables 1 and 2 respectively.

Table 1: Properties of conventional binder 50/70 used to prepare asphalt specimens for CRS test at VTI.

	Result	Standard
Softening point (°C)	50.4	EN 1427 [27]
Penetration at 25°C (0.1 mm)	59	EN 1426 [28]

Table 2: Properties of Polymer modified binder PMB 45 / 80 – 65 used to prepare asphalt slabs for CRS test at VTI.

	Result	Standard
Softening point (°C)	64.5	EN 1427 [27]
Penetration at 25°C (0.1 mm)	62	EN 1426 [28]

2. 2. Aggregates

The required quantities of each type of aggregate used for the CRS test have been sent to VTI from UC in Spain as described below. In ALTERPAVE project, it has been recommended to fulfil the standard grading limits (in volume percentage) considering, first of all, the RAP gradation, secondly, the by-products gradation and lastly the natural aggregates gradation. The approach considered in the ALTERPAVE project entails that the alternative and natural aggregate should comply with the same technical requirements. The requirements that are demanded for the coarse and fine aggregate vary with the specific country in Europe, more details about the technical and Environmental requirements on the materials used in this project is given in Kuttah et al. [29].

2. 2. 1. Natural aggregates

The Spanish Ophitic aggregate has been used as the course aggregate in some mixtures, while the limestone aggregate has been used as the fine aggregate and filler. Note that the percentage of natural aggregates in some alternative mixtures were less than 2%.

2. 2. 2. By-Products aggregate

Different types and percentages of alternative materials have been used in preparing the asphalt samples for the CRS tests including reclaimed asphalt pavement (RAP), electric arc furnace (EAF) slag, basic oxygen furnace (BOF) slag and foundry sand.

2. 3. Rejuvenators

Rejuvenators are used to mitigate the effect of the changes in chemical and physical properties of the asphalt binder due to in-service aging and restore some of the properties of the aged binder in the RAP. The maximum RAP percentage adopted in this study was about 35%, correspondingly, it has been decided to use rejuvenators in order to reinstate the penetration grade of the aged asphalt binder to the target penetration grade of the new neat asphalt binder for a given application.
Four types of rejuvenators used as additives were examined in ALTERPAVE projects, two of them has been selected to be used for the mixtures prepared for the circular road simulator test at VTI. These two rejuvenators are bio-oils (plant-based), namely RS and RVE.

3. Mixtures summary

Based on the laboratory tests carried out at UC and discussed in detail in Kuttah et. al. [29], Tables 3 and 4 below illustrates a summary of the composition of sixteen asphalt mix designs developed with the recommended percentages of binder contents.

Table 3: A summary of aggregates composition of asphalt mixtures

Mix. No.	EAF slag (%)	BOF slag (%)	Ophiti Agg.[1] (%)	RAP (%)	F-sand[2] (%)	Lime - stone (%)	Rejuv.[3]
M01	50.5	-	-	35.5	12.1	1.9	RS
M02	60.5	-	-	21.7	14.9	2.9	RS
M03	-	50.1	-	35.3	12.8	1.8	RS
M04	50.1	-	-	35.3	-	14.6	RS
M05	59.9	-	-	21.5	-	18.6	RS
M06	-	-	44.10	39.5	-	16.4	RS
M07 old	50.5	-	-	35.5	12.1	1.9	RVE
M07 new	50.5	-	-	35.5	12.1	1.9	RVE
M08	60.5	-	-	21.7	14.9	2.9	RVE
M09	-	50.1	-	35.3	12.8	1.8	RVE
M10	50.1	-	-	35.3	-	14.6	RVE
M11	59.9	-	-	21.5	-	18.6	RVE
M12	-	-	44.10	39.5	-	16.4	RVE
M13	50.5	-	-	35.5	12.1	1.9	-
M14	76.3	-	-	-	19.2	4.5	-
R01	-	-	66.50	-	-	33.5	-
R02	-	-	66.50	-	-	33.5	-

[1] Ophitic aggregate
[2] Foundry sand
[3] Rejuvenator

Table 4: A summary of binder characteristics of the asphalt mixtures

Mix. No.	Neat binder per weight (%) EN 12697-39 [30]	RAP binder per weight (%)	Total binder per weight (%) EN12697-39 [30]	Neat binder per volume (%)	RAP binder per volume (%)	Total binder per volume (%)	Bulk density (Mg/m^3) EN 12697- 6 [31]
M01	3.2	1.4	4.6	8.6	3.9	12.5	2.805
M02	3.3	0.9	4.2	9.1	2.4	11.6	2.848
M03	3.4	1.4	4.8	8.4	3.6	12.0	2.59
M04	2.4	1.4	3.8	6.3	3.9	10.2	2.775
M05	2.9	0.9	3.8	8.1	2.4	10.5	2.87
M06	2.2	1.6	3.8	5.2	3.9	9.1	2.481
M07 old	3.2	1.4	4.6	8.4	3.9	12.3	2.649
M07 new	3.2	1.4	4.6	8.4	3.9	12.3	2.759
M08	3.8	0.9	4.7	10.5	2.4	12.9	2.84
M09	3.9	1.4	5.3	9.7	3.6	13.2	2.582
M10	2.4	1.4	3.8	6.3	3.9	10.2	2.777
M11	2.7	0.9	3.6	7.5	2.4	9.9	2.859
M12	3.0	1.6	4.6	7.2	3.9	11.0	2.482
M13	3.3	1.4	4.7	8.9	3.9	12.8	2.802
M14	4.5	0.0	4.5	13.0	0.0	13.0	2.983
R01	4.3	0.0	4.3	10.5	0.0	10.5	2.522
R02	4.3	0.0	4.3	10.4	0.0	10.4	2.498

Note that the aggregate composition of the mixtures from M01 to M06 is the same as for mixtures from M07 to M12, but the only difference is the type of the rejuvenator used.
Since it is possible to test only twenty-eight asphalt slabs simultaneously using the VTI's circular road simulator, fourteen asphalt mixtures have been chosen among the mixtures given in Table 3, namely, M01, M02, M03, M04, M05, M06, M07, M08, M010, M011, M012, M013, Reference 01, and Reference 02. Two identical asphalt slabs were prepared for each chosen mixture and tested using the VTI's CRS.

4. The circular road simulator test

Under controlled conditions, the CRS implements an accelerated test that simulate the effect of traffic on pre- manufactured slabs of different types of roads materials (specially asphalt coatings) to record the corresponding wear, deformations and texture developments under different loading and environmental conditions, see Figure1. Furthermore, the CRS test has been used to link the laboratory test results to the field observations and to assess the impacts of new tires, tire inflation pressures, load limits, etc on the asphalt mixtures or other road materials.
The VTI's CRS has six axles (of which four wheels are in operation) running on a circular test track. A separate DC motor is driving each wheel and the speed can reach up to 70 km h-1. The diameter of the track is 5.25 m, giving an average track length of about sixteen meters. The maximum width of the track is about 0.85 m. The track consists of twenty-eight test slabs that can be manufactured in the Lab. Before the test stars, the axles are lowered down, and the desired axle loads are achieved. Moreover, the temperature and relative humidity in the simulator hall can be controlled via an internal air cooling system. The temperature in the hall can be varied from -5 to + 40 ° C and during the test, the samples surfaces can be sprinkled with water. The measurements of cross sections made with a laser profile measurement beam that can provide more than 400 data points per slab with 0.01 mm accuracy. For each tested slab, three cross sectional profiles are usually measured.

In addition, one of the wheels is provided with texture development measurement indicators to measure the mean profile depth (MPD) along the track.
As highlighted previously, a total of fourteenth asphalt mixtures have been tested at VTI testing facility. Twelve of these asphalt mixtures contained industrial wastes in different compositions and quantities, while the other two mixtures were made totally of natural materials for comparison purposes.
In this study, the CRS test has been used to assess the surface deterioration, wear and the changes in macrotextures of the tested asphalt slabs under wheel loading in dry or wet conditions and under different testing temperatures to simulate summer and winter seasons. In addition, studless and studded tires have been used to traffic the asphalt slabs during the CRS testing in order to simulate the current roads conditions in different European countries since many countries permit the use of studded tires during winter for safer winter driving; e.g. Sweden, Finland, Denmark, Norway, France, Ireland, and other countries.

Fig. 1: The VTI's Circular Road Simulator, photo after VTI Image Database, 2016

Table 5: The CRS Testing Program.

The phase nummber	Phase period (Duration)	The total number of revolutions in each phase	The measurements have been carried out at the end of the following accumelative number of	Type of the measurment		Type of the tire	Testing temperature (C°)	Wheel Speed (km/h)	Testing with or without sprinkling of water
				Profile	Texture				
One	Very short phase (Pre-loading)	2000	100	Yes	Yes	Studless (winter tire)	0	30	without water
One			2000	Yes	Yes				
Two	Long phase	168000	40000	Yes	Yes	Studless (summer tire)	30	60	without water
Two			122000	Yes	Yes				
Two			170000	Yes	Yes				
Three	Medium-Long phase	120000	210000	Yes	No	Studless (winter tire)	Started with -2 (the test temperature should not exceed +2 during the test)	70	Daily, the test is started in the morning at dry conditions for the first few revolutions. Afterward the water is added and the test proceeds . At the end of the day, the water is discharged. This procedure was repeated for 5 to 6 consecutive days.
Three			290000	Yes	Yes				
Four	Medium-Long phase	90 000- 120000	380000	Yes	Yes	Studded tire	Started with -2 (the test temperature should not exceed +2 during the test)	70	The same as for phase three

4. 1. General test preparation

The CRS has been carried out according to the testing program described in Table 5. The selected fourteen asphalt mixtures have been prepared in the pavement technology laboratory at VTI under controlled conditions following the adopted mix designs described in Table 3 above.
During the manufacturing of the asphalt mixtures the natural and alternative aggregates (except the RAP) were heated up to 185°C for 5.5 hours approximately. The RAP was heated up to 110°C for a maximum time of 2 hours. When the RAP had been taken out of the oven, the rejuvenator was poured above it with a little sprayer directly in the mixer drum. The asphalt binder was heated up to 150°C for approximately 3 hours and then added to the mixture. The mixer drum was previously heated at 150°C (the same temperature of the asphalt binder). Then all the aggregates and asphalt binder mixed for about 5 minutes, although the time depends on the quantity and the type of sample to be manufactured.
After preparing the fourteen selected mix designs, two asphalt slabs of each mixture have been prepared and compacted in rectangular steel slabs each having a dimension of (750 * 480* 40) mm. The preparation of each asphalt plate has been started by heating the asphalt mixtures to the desired temperature in a huge oven at VTI's facility and placing the desired quantity of the asphalt mixture under consideration in the middle of the steel mould and then spread the asphalt mixture to fill in the steel mould.
Then, a roller compactor has been used to compact and force all the desired asphalt mixture inside the steel plate, see Fig.2 A.
After removing each asphalt plate from its mould, the asphalt slabs have been sawed to trapezoidal shapes to fit the circular path of the CRS and then dried, see Fig 2 B. Then, all the twenty-eight asphalt slabs glued on the circular track by a special glue. Asphalt slabs with expected similar wear resistance have been placed side by side to reduce the expected differences in surfaces' levels between the adjacent asphalt slabs during testing and hence minimize the jumping of the machines wheels during operation, see Fig.2 C. The joints between the slabs have been sealed with a sealing mixture.

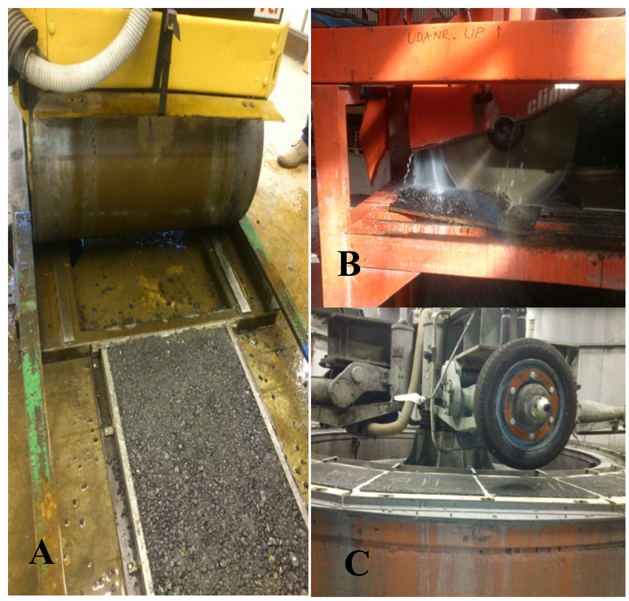

Fig. 2: CRS test preparation, A- compacting the asphalt slabs, B- sawing the asphalt slaps, C- fitting and gluing of the asphalt slabs on the circular track of the CRS

4. 2. Measurements related to CRS test

Surface deformations, wear and macrotexture measurements have been taken at various traffic intervals during the CRS test according to the schedule given in Table 4.
The surface deformations and wear measurements have been taken by passing a laser beam over three predefined lines on the surface of each tasted asphalt plate fixed on the CRS track. The laser beam measures the deformations along these lines after predetermined traffic intervals. The surface deterioration or wear has been determined as the difference between the profile at zero CRS revolutions and the profile after a predetermined number of CRS revolutions.

The macrotextures of the tested asphalt slabs have been measured in terms of mean profile depth values (MPD) using a laser texture scanner system after predetermined traffic intervals applied using the circular load simulator. According to ISO 13473-2 [32], the pavement macrotexture is characterized by a deviation of a pavement surface from a true planar surface with the characteristic dimensions along the surface of 0.5 mm to 50 mm, corresponding to texture wavelengths with one-third-octave bands including the range 0,63 mm to 50 mm of center wavelengths.
The used device scans the material surface to measure the mean profile depth (MPD) which is defined as the average value of the profile depth over a 100-mm long baseline.

5. Testing results and discussion

The results of the CRS test have been analysed to evaluate the technical performance of the alternative asphalt mixtures as compared to the performance of the control conventional mixtures. As described previously, various measurements have been considered during the accelerated CRS testing. The results corresponding to these measurements are described and discussed below:

5.1. Surface deterioration and wear measurements results

In order to get a good correlation between the number of CRS revolutions and the type of the mixture, the average surface deterioration and wear of each two identical asphalt slabs (i.e. made of the same mix design) has been considered and hence the results have become more correlated to the type of the mix, as presented in Fig.s 3 and 4.
Note that the profile measurements have been carried out more frequently at the beginning of the CRS test and less frequently during the course of the test. The surface deterioration and wear measurements given in this study represent those measured under the wheel only and not for the whole width of the slabs.
Fig. 3 shows the correlation between the type of the asphalt mixture and the corresponding surface deterioration after different CRS traffic intervals up to 290 000 revolutions, during which, the summer and winter conditions in European countries have been simulated using summer and winter friction tiers.
In Fig. 3, the surface deteriorations refer to the difference in the profiles after the polishing phase (at the end of phase 1 after 2000 CRS revolutions) and the profile after a predetermined number of CRS revolutions using studless tires (i.e. to the end of phase 3 at 290000 CRS revolutions).
It can be seen from this figure that in terms of surface deterioration the asphalt slabs of R1 (reference mixture of natural materials) has performed best, but some of the asphalt slabs made of by-products materials, namely mixtures 12 and 7 old, have performed as well as R2 (the other reference mixture). Note that at the end of 290 000 CRS revolutions, the surface deteriorations reported for mixtures 12, 7 old and 1 were only 0.5 mm (or less) higher than the surface deterioration reported for mix R1.
Regarding the ability of the developed asphalt mixture to resist the wear caused by studded tires used in Nordic European countries during winter, Fig. 4 illustrates the effect of the number of CRS revolutions with studded tires on the wear characteristics of the different asphalt mixtures. The wear shown in Fig. 4 refers to the changes in profile and the corresponding deterioration took place only during the fourth phase of the CRS traffic loading (i.e. between 290 000 and 380 000 CRS revolutions) where studded tires were used.

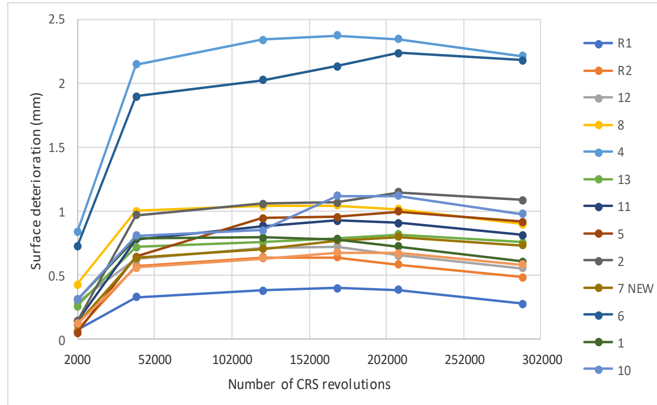

Fig. 3: Effect of CRS traffic on the surface deterioration characteristics of the tested asphalt mixtures.

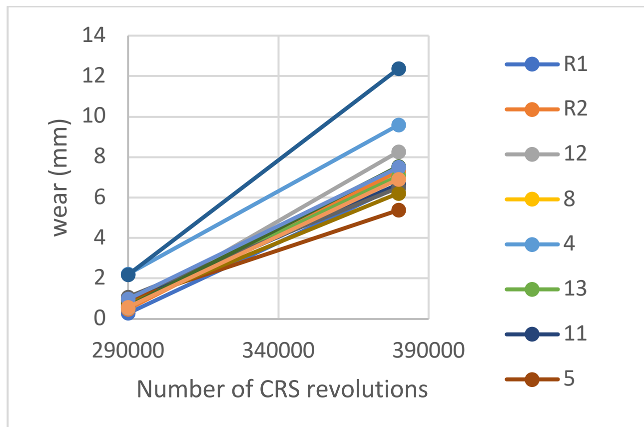

Fig. 4: Effect of CRS traffic on the wear characteristics of the tested asphalt mixtures.

It can be seen from this Fig. 4 that asphalt mixtures made of by-products (industrial wastes) showed very good resistance against loading with studded tires and some of them performed even better than the reference asphalt mixtures made totally of natural materials. According to Fig. 4, the best performed mixtures are mix 5 followed by mixtures 2, 7 new, 8, 11, R1, 13, 7old, 10, R2, 1, 4, 12 and 6 in sequence.

5.2. Macrotexture scanning results

The MPD values have been measured on the surfaces of the tested asphalt slabs at the end of 0, 2000, 40000, 122000, 170000, 290000, and 380000 CRS revolutions according to the testing program described previously in Table 4.
To reduce, as much as possible, the effect of RAP and manufacturing characteristics on the MPD values of the two asphalt slabs made of the same mix design and to get a good correlation between the number of CRS revolutions and the type of the mixture, the average MPD values of each two identical asphalt slabs (i.e. made of the same mix design) has been considered and hence the results have become more correlated to the type of the mix.
Fig. 5 shows the correlation between the type of the asphalt mixture and the MPD values after different CRS traffic intervals up to 290 000 revolutions, during which, the summer and winter

conditions in European countries have been simulated using summer and winter friction tiers.

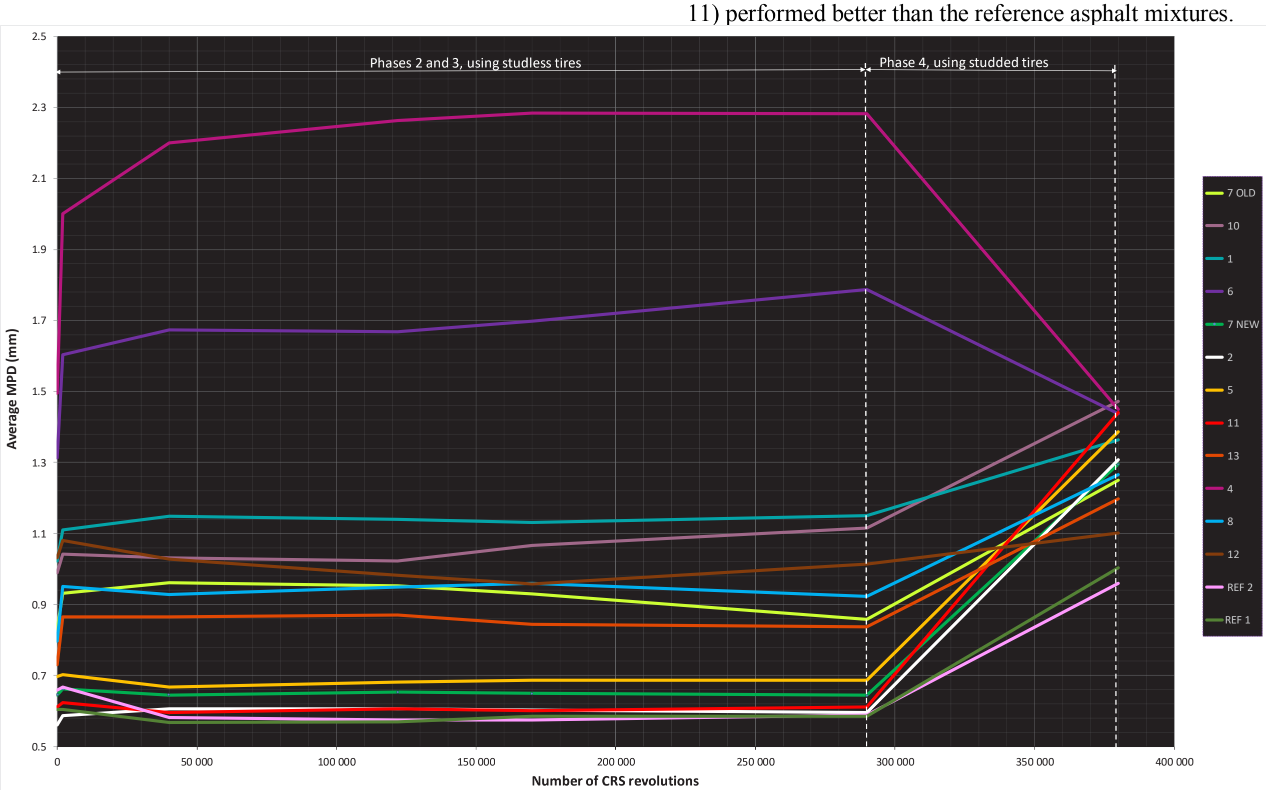

Fig. 3: Correlation between the average MPD values and the number of CRS revolutions for the tested asphalt mixtures.

It can be concluded from Fig. 5, that the changes occurred in the MPD values of the asphalt slabs between 2000 CRS revolutions and 290 CRS 0000 have been lowest for mixtures 2, 7 new, 13, 11, 5, R1 and 1. This means that these mixtures have resisted best the changes in its macrotextures due to trafficking with studless tires based on the average MPD data.
Moreover, the mixtures that have resisted best the changes in their macrotextures under studded tires (usually used during winter in Nordic European Countries) traffic loading between 290000 CRS revolutions and 380 000 revolutions (during the fourth phase), have been considered as the best based on MPD values evaluation. Considering this definition, the best mixtures with minimum changes in their MPD values during the fourth phase of CRS traffic loading have been mixtures 12, 1, 8, 6, 10, 13, R2, 7 old, R1, 7new, 5, 2, 11, 11 and 4 in sequence.

6. Conclusions

It can be concluded from this study that by controlling the homogeneity of recycled material and by using rejuvenators with adequate quality, it is possible to obtain paving mixtures with high content of recycled materials (up to 98%) that can substitute conventional asphalt mixtures made of natural materials.
Based on the CRS test results, it has been noticed that the asphalt slabs of R1 (reference mixture of natural materials) has performed best, but some of the asphalt slabs made of by-products materials, namely mixtures 12 and 7 old, have performed as well as R2 (the other reference mixture). Regarding the ability of the new developed asphalt mixture to resist the wear caused by studded tires used in Nordic European countries during winter, it has been observed that some asphalt mixtures made of high percentages of by-products (namely mixture 5 followed by mixtures 2, 7 new, 8, 11) performed better than the reference asphalt mixtures.

With respect to the macrotextures properties of the tested asphalt mixtures, it can be concluded that the changes occurred in the MPD values of the asphalt slabs loaded from the beginning of phase 2 to the end of phase 3 (i.e. from 2000 CRS revolutions to 290 0000 CRS revolutions) have been lowest (and hence better) for the Alternative mixtures 2, 7 new, 13, 11, 5, as compared to the reference mixtures R1 and R2. In addition, the mixtures that have resisted best the changes in their macrotextures under studded tires' traffic loading during the last phase (i.e. between 290000 CRS revolutions and 380 000 revolutions) with minimum changes in their MPD values during the fourth phase of CRS traffic loading have been also those made of high percentages of by- products namely mixtures 12, 1, 8, 6, 10, 13.

Acknowledgment

This paper is based on the work done in the framework of ALTERPAVE European project https://www.giteco.unican.es /proyectos/ALTERPAVE/index.htm. The author would like to thank the European Commission for their financial support of ALTERPAVE project-31109806.0006 through the Infravation Funding Program. Furthermore, the author would like to thank ALTERPAVE project partners, namely from University of Cantabria- the project coordinator- (Spain), Western Research Institute (USA), Acciona (Spain) and Impresa Bacchi (Italy) for the effective business communication throughout the project.

List of abbreviations

BOF	Basic oxygen furnace slag
CRS	Circular road simulator
EAF	Electric arc furnace slag
MPD	Main Profile Depth
PMB	Polymer modified asphalt binder
RAP	Reclaimed Asphalt Pavement
UC	University of Cantabria
VTI	The Swedish National Road and Transport Research Institute

References

[1] European Aggregates Association annual review 2016-2017 http://www.uepg.eu/uploads/Modules/Publications/uepg-ar2016-17_32pages_v10_18122017_pbp_small.PDF, Brussels, Belgium, 2017.
[2] Y. Huang, R. N. Bird, and O. Heidrich, "A review of the use of recycled solid waste materials in asphalt pavements," Resources, Conservation and Recycling 52, pp.58–73, 2007.
[3] J. A. Epps, "Uses of recycled rubber tyres in highways," Washington, DC: Synthesis of Highway Practice No.198, TRB National Research Council. NCHRP Report, 1994.
[4] X. Shu, and B. Huang, "Recycling of waste tire rubber in asphalt and portland cement concrete: An overview," Construction and Building Materials 67, pp.217–224, 2014.
[5] P. Lastra-González, M. Calzada-Pérezb, D Castro-Fresnoa, and I. Indacoechea-Vegaa, "Asphalt mixtures with high rates of recycled aggregates and modified bitumen with rubber at reduced temperature, Road Materials and Pavement Design," DOI:10.1080/14680629.2017.1307264, 2017.
[6] A. Farina, M. C. Zanetti, E. Santagata, and G. Blengini, "Life cycle assessment applied to bituminous mixtures containing recycled materials: Crumb rubber and reclaimed asphalt pavement," Resources, Conservation and Recycling 117, pp. 204–212, 2017.
[7] I. L. Al-Qadi, M. A. Elseifi, and S. H. Car "Reclaimed Asphalt Pavement – A Literature Review," Illinois Center for Transportation, Urbana (IL), USA (2007), Report No.: FHWA-ICT-07-001., 2007.
[8] T. Jacobson, and A. Waldemarson, "Warm recycling in asphalt plant – Test of binder layer on Road 40," Rya–Grandalen, VTI notat 21-2008, Linköping, Sweden (In Swedish), 2008.
[9] D. Kuttah, E. Nielsen, A. Pettersson, and M. Tušar, "Production and Processing of Reclaimed Asphalt - Selected case studies," European project report, Deliverable 4.4 Re-Road Project. http://re-road.fehrl.org/?m=48&id_directory=7325, 2012.
[10] I. Carswell, R. Karlsson, J. Raaborg, and D. Kuttah, "Main Report on Results of Comparative Site Monitoring," European project report, Deliverable 2.6, Re-Road Project. http://re-road.fehrl.org/?m=48&id_directory=7325, 2012.
[11] H. Al-Bayati, S. Tigheb, and J. Achebec. "Influence of recycled concrete aggregate on volumetric properties of hot mix asphalt," Resources, Conservation & Recycling 130, pp.200–214, 2018.
[12] N. Su, and J. S Chen, "Engineering properties of asphalt concrete made with recycled glass," Resourc Conserv Recycl 35, pp.259–74, 2002.
[13] U. Bagampadde, H. Wahhab, S. Aiban, "Optimization of steel slag aggregates for bituminous mixes in Saudi Arab," J Mater Civil Eng., pp. 30–5, 1999.
[14] M. I. Khan, and H. Wahhab, "Improving slurry seal performance in eastern Saudi Arabia using steel slag," Construct Build Mater 12, pp.195–201, 1998.
[15] S. Wu, Y. Xue, Q. Ye, and Y. Chen, "Utilization of steel slag as aggregates for stone mastic asphalt (SMA) mixtures," Building and Environment 42, pp.2580– 2585, 2007.
[16] M. Ergun, S. Iyinam, A. F. Iyinam, "Flexural behavior of waste plastic added asphalt concrete mixture," in proceedings of the International Symposium on Pavement Recycling, 2005.
[17] E. Ahmadinia, M. Zargar, M. Karim, M. Abdelaziz, and E. Ahmadinia, "Performance evaluation of utilization of waste Polyethylene Terephthalate (PET) in stone mastic asphalt," Construction and Building Materials 36, pp. 984–989, 2012.
[18] T. Kütük-Sert, and S. Kütük, "Physical and Marshall Properties of Borogypsum Used as Filler Aggregate in Asphalt Concrete," Journal of Materials in Civil Engineering 25 (2), pp.266-273, 2013.
[19] D. Kuttah, K. Sato, and C. Koga, "Evaluating the Dynamic Stabilities of Asphalt Concrete Mixtures Incorporating Plasterboard Wastes," International Journal of Pavement Engineering 16 (10), pp.929-938, 2015.
[20] J. W. Button, D. Williams, and J. A. Sherocman, "Roofing Shingles and toner in asphalt pavements," FHWA Research Report, FHWA/TX-96/1344-2F, Texas Transportation Institute, 1996.
[21] K. Foo, D. I. Hanson, and T. Lynn, "Evaluation of Roofing Shingles in Hot Mix Asphalt," Journal of Materials in Civil Engineering 11 (1), DOI 1061/(ASCE)0899-1561(1999)11:1(15), 1999.
[22] S. Burak, and T. Ali, "Use of asphalt roofing shingle waste in HMA," Construction and Building Materials 19 (5), pp. 337–346, 2005.
[23] K. H. Moon, A. C. Falchetto, M. Marasteanu, and M. Turos, "Using recycled asphalt materials as an alternative material source in asphalt pavements," KSCE Journal of Civil Engineering 18 (1), pp.149–159, 2014.
[24] Z. You, J. Mills-Beale, X. Yang, and Q. Dai, "Alternative Materials for Sustainable Transportation," Michigan Department of Transportation, Final Report 11/13/2009 -12/31/2012, RC-1591, 2012.
[25] R. West, A. Kvasnak, N. Tran, B. Powell, and P. Turner, "Testing of Moderate and High Reclaimed Asphalt Pavement Content Mixes," Transportation Research Record: Journal of the Transportation Research Board, No. 2126, Transportation Research Board of the National Academies, Washington, D.C., 100–108, DOI: 10.3141/2126-12., 2009.
[26] J. Bukowski, J. Youtcheff, and T. Harman, "An Alternative Asphalt Binder, Sulfur-Extended Asphalt (SEA)," U.S. Department of Transportation, Federal Highway Administration, Office of Pavement Technology, FHWA-HIF-12-037, 2012.
[29] D. Kuttah, I. Indacoechea, I. Rodríguez, P. Lastra González, E. Blas, R. Casado, R. Boysen, J. Planche, and L. Trussardi, "ALTERPAVE Methodology," Deliverable 5.2, ALTERPAVE European project report, 2018.
[28] EN 1426, "Bitumen and bituminous binders - Determination of needle penetration", 2015
[27] EN 1427, "Bitumen and bituminous binders - Determination of the softening point - Ring and Ball method2, 2007.
[30] EN 12697-39, "Bituminous mixtures - Test methods for hot mix asphalt - Part 39: Binder content by ignition", 2013.

[31] EN 12697-6, “Bituminous mixtures - Test methods for hot mix asphalt - Part 6: Determination of bulk density of bituminous specimens”, 2012.
[32] ISO 13473-2, “Characterization of pavement texture by use of surface profiles — Part 2: Terminology and basic requirements related to pavement texture profile analysis”, 2002.

Journal of Geotechnical and Transportation Engineering
Volume 4 | Issue 1
Autonomous Vehicles: Rethinking Traffic Congestion Solutions in Cities
Iravani et al.
Received 5/15/2018 Accepted 6/1/2018
Published 7/1/2018
Corresponding Author:
Hamid Iravani;
hamid.iravani@parsons.com
www.jgtte.com

Autonomous Vehicles: Rethinking Traffic Congestion Solutions in Cities

Hamid Iravani
Transportation Planning Director, Fellows Board Member Parsons, Dubai, United Arab Emirates
Email: hamid.iravani@parsons.com

Adrian Anderson
Senior Civil Engineer, Parsons, Dubai, United Arab Emirates
Email: adrian.anderson@parsons.com

Andrew Bevan
Smart Mobility Director, Parsons, Dubai, United Arab Emirates
Email: andrew.bevan@parsons.com

Abstract

Autonomous vehicles (AVs) will be the next technological leap for urban mobility. The question for decision makers and city leaders is whether they contribute to achieving progressive social, environmental, and economic targets or achieve the opposite. AVs offer benefits such as safety, convenience, and enhanced mobility for the young, the elderly, and the disabled. However, AVs themselves will not relieve traffic congestion and in fact could exacerbate traffic and increase vehicle miles traveled (VMT) unless clear regulations and policies are adopted to manage their use. In this paper, we outline the four transport planning tools that are used to relieve traffic congestion: (1) land use measures, (2) transportation demand management, (3) transportation system management, and (4) road widening/new roads. We address how AVs will complement or disrupt the effective use of these tools and conclude that the tools must be overhauled with the advent of automated mobility. Policy recommendations are provided for each tool. In addition, we briefly discuss the new safety challenges posed by integrating AVs into traffic.

Keywords: Autonomous Vehicles; Transportation Demand Management; Transportation System Management; Sprawl

1. Introduction

Land use and transportation are inseparably linked. Throughout history, any advancement in transportation technology has had major impacts on travel patterns and urban form. Following the advent of the automobile in cities where policies did not intervene, higher speed and more efficient vehicles brought urban sprawl. Residents began to live far from city centers and drive farther to work. Although car-oriented cities benefited a portion of their populations, they created adverse economic, environmental, and social impacts for the majority.

Mainstream car manufacturers already boast of semiautonomous driving technology built into some high-end vehicles. Level 5 autonomous vehicles (AVs), which can operate in mixed traffic scenarios, are being tested in several locations throughout the world. Many urban developments and road layouts are already lagging in addressing the changes that AVs will bring. Their use will reshape cities, and it is imperative that decision makers also overhaul policies to ensure that we maximize the efficiencies of this technology.

A revolution in urban mobility will revolutionize a city's future development. Girardet [1], co-founder of the World Future Council, raised the concept of two opposing city types. First, the dystopian "Petropolis," a geographically spread-out city that relies on fossil fuels, has a high urban metabolism and large ecological footprint. Second, the utopian "Ecopolis," a compact, "regenerative" city based on a circular economy with a smaller geographic and ecological footprint. A Petropolis with high urban sprawl is less efficient not only because of the greater distances traveled in vehicles, but also because of the greater energy used to transport water, wastewater, and other commodities. It is taken as fundamental in this paper that mobility of the future should be a catalyst to transform cities away from the traffic congestion, fossil fuel dependence, air pollution, and urban sprawl associated with a Petropolis.

Within the emerging field of automated mobility, a battle of ideas has arisen between those developing private AVs (self-driving cars, typically from automobile manufacturers) and those advocating nonmotorized and public transit modes. This paper focuses on how the unregulated advance of private AVs will affect the four tools that are commonly used to combat congestion and briefly discusses the new safety challenges posed by integrating AVs into traffic. It concludes by describing how these strategies must adapt to ensure that the future state of cities is liveable and sustainable.

2. Impact of Transportation Technology Advancement on Urban Form

Transportation has been the framework upon which cities are formed. Land use and transportation are interconnected: change in one influences change in the other. In his notable book, *The Ways of the World*, Maxwell Lay [2] provides a history of the evolution of transportation technology from the earliest footpaths to the rise of wheeled vehicles and animals to pull them, the development of surfaced roads, the motivation behind building roads and bridges, and the advent of cars and their impact on roads, cities, and society in general. Lay highlights three distinct eras: ancient times, the Industrial Revolution (ca. 1825–1900) and the private motor vehicle era (1925–present). Each era is distinguished by a different transportation technology and a correspondingly different urban form.

In ancient times, the main modes of transportation were by foot or animal. As a result, land uses were centralized for better accessibility and connectivity. The Industrial Revolution brought higher speed streetcars, subways, elevated rail, and commuter rail lines that replaced the horse-drawn cars and enabled residents to live farther from urban centers and thus reduced population densities while main land use activities centered on transit stations. Finally, the private motor vehicle era spread land use activities beyond the walking distance to transit stops or stations. From 1916 to 1920, automobile ownership increased from 2 million to 8 million; by the beginning of World War II (1940), the United States alone had 32.45 million motor vehicles. After World War II, the U.S. Federal-Aid Highway Act of 1956 authorized the construction of 41,000 miles of high-speed freeways and expressways. By 1972, these roads would connect 90 percent of the cities with a population of 50,000 or more. They were also built to link many smaller cities, which resulted in the development of low-density suburbs that could only be served by cars. Urban areas expanded and encroached on agricultural areas far beyond city limits [3]. Most European cities had road layouts that were based on transportation by foot or animal and thus struggled to cope with the advent of cars.

In general, any advancement in transportation technology that led to higher speed resulted in a separation of land use activities and changed settlement arrangements. Urban sprawl resulted in higher vehicle miles traveled (VMT) and greater traffic congestion, which, in turn, resulted in more pollution and greater energy consumption and cost. Cities became less transit oriented and less walkable to such an extent that they even harmed the health and well-being of the population they supported. AVs are also expected to significantly affect the shaping of the physical, social, and economic gradients of cities. Below we describe why and how the four tools to address traffic congestion must adapt to AVs.

3. Four Tools to Alleviate Traffic Congestion

To alleviate traffic congestion, urban municipalities commonly use four tool categories:

- Tool 1: Apply land use measures for mixed-use, compact, and high-density development. Such land use measures are effective because traffic is the manifestation of land use, thus they target the cause of traffic.
- Tool 2: Implement transportation demand management (TDM) to shift modes from private automobiles to public transit and high-occupancy vehicles (HOV).
- Tool 3: Implement transportation system management (TSM) to optimize the current arrangement and manage traffic more efficiently.
- Tool 4: Widen roadways and add new roads and parking. These measures attempt to ease traffic congestion by managing the supply side of transportation and extending physical infrastructure.

4. AV Impact on Tool 1: Improve Traffic by Applying Land Use Measures

Travel is a derived demand; trips are generated as a result of land use activities. The most effective tools to alleviate traffic congestion are those that address the causes rather than the effects. Mobility within a city must satisfy various trip purposes, but the distance at which mobility is required can be reduced. Land use measures, including mixed-use, compact, and high-density developments, make such reduction possible. These measures bring origins closer to destinations and thus reduce the VMT. A risk is that the convenience provided by AVs will increase the distance that passengers are willing to travel, which conflicts with the goal of compact and high-density development.

The Arizona Department of Transportation [4] conducted extensive research on the relationship between higher density development and traffic congestion. The research also refers to a variety of studies that indicate that higher density developments result in ownership of fewer cars and in households that drive less, walk more, and take more trips on public transit. On average, the daily VMT generated by households for higher density developments is one-half to one-third of the daily VMT of their suburban counterparts. The study also concluded that travel behavior is affected by land use factors such as mixed-use development, automobile versus pedestrian-oriented design, and regional accessibility enhanced by multiple travel choices (especially transit); these factors are effective in improving traffic. These characteristics—density, diversity, design, and destination—are known as the 4Ds. The travel market that may be most influenced by compact mixed-land use is nonwork travel. Real estate industry experts state that more compact, mixed-use development has not occurred because of restrictive local zoning codes or traffic level of service standards rather than because of market demand. Visual preference surveys indicate a general preference for older (pre-World War II) suburban development patterns: these developments are more compact and walkable, and they foster more social interaction among residents. In addition to improved mobility, compact cities consume less water and energy than do sprawling Ecopolis-model cities.

In many cities, rules and regulations have not been amended to address congestion, and the higher speed and greater efficiency of cars has encouraged populations to live in low-density suburbs away from activity centers, which has resulted in urban sprawl. AVs will also bring higher speed (due to less delay in traffic flow as the result of steady flow of platooning vehicles), but more importantly, the convenience of AVs will enable travelers to drive longer distances in a high level of comfort, and they can work or rest in the vehicle. This will encourage residents to live farther from urban centers and will encourage developments to grow horizontally, which will decrease accessibility to public transit, increase infrastructure requirements, and reduce farmland and natural areas. Policies and regulations must be enacted to curtail the negative impacts of AV on urban form.

5. AV Impact on Tool 2: Improve Traffic by Implementing Transportation Demand Management

TDM is a series of measures that emphasizes the mobility of people and goods rather than cars and includes measures to promote walking, cycling, ridesharing, public transit, and telecommuting. TDM's effectiveness depends on the availability of modes other than single occupant vehicles (SOVs) and policies to encourage their use. To estimate mode shares, discrete mode choice models traditionally use the observed modal attributes of alternatives (e.g., travel time and cost), and characteristics of commuter sociodemographic (e.g., household income and number of drivers in a household). These models have not paid much attention to the unobserved attributes, such as the effect of convenience and comfort on choosing a mode of transportation.

Mode choice models in transport planning should be improved by considering the often-ignored location-specific and latent variables in addition to the conventional ones. A study conducted by Alex et al. [5] identified five latent variables: (1) mode comfort and convenience, (2) commuter habits, (3) mode safety, (4) commuter life cycle, and (5) mode reliability. Johansson et al. [6] have proven that mode choice decisions also depend on commuters' preferences for convenience, safety, or flexibility. In several examples, a "latent variables enriched" model outperforms a traditional model and offers insight into the importance of these latent variables in mode choice. In general, the results confirm that time and cost are significant for mode choice, but they also indicate that preferences for flexibility and comfort are very important.

One of the main objectives of the automotive industry in the advent of automation is to increase sales by focusing on enhanced comfort and convenience for travelers. AVs will allow travelers to work—and rest—while traveling. AVs can remove the inconvenience associated with searching for parking spaces. Moreover, AVs serve those who cannot drive, such as the young, the elderly, or the disabled. In choosing AVs over other modes of transportation, the importance of convenience and comfort are location specific and will vary among socioeconomic groups, but in many studies, comfort and convenience were listed as the prime factor in mode choice. These criteria play an important role in determining the mode choice and encourage the use of private AV modes rather than public transit. The result will adversely affect future traffic unless authorities make policy decisions to prioritize societal interest over individuals. Cities have witnessed the same effect from automobiles. Although private automobiles have enhanced individual comfort and convenience, in the absence of best practice planning and smart growth measures, they have negatively affected the quality of life and, in many urban areas, they have prioritized the automobile above the people they are meant to serve.

AVs will provide mobility for those who cannot drive (e.g., the young, the elderly, and the disabled), thus generating new roadway demands. This segment of demand currently uses modes other than SOVs; as a result, the VMT relating to this segment of demand will rise. On the positive side, public AVs will promote car sharing for regular travel, especially for commuting, thus reducing overall car ownership and vehicle travel, especially in compact urban areas. Carlo Ratti, Director of MIT's Senseable City Lab, predicts that vehicle automation will require 80 percent fewer cars on any given highway. He states, "In general, fewer cars could mean shorter travel times, less congestion, and smaller environmental impact," but he also warns of nightmarish scenarios. If private AVs were to become significantly cheaper than public transit, cities could easily become gridlocked [7]. This echoes the earlier observation that policies and legislation must grow at the same rate as technology to ensure that we are not prisoners of the AV era and that we do not lose the ability to influence the modal shift to public mass transit options.

6. AV Impact on Tool 3: Improve Traffic by Implementing Transportation System Management

TSM relates to the measures that optimize existing infrastructure performance by preserving capacity and improving the security, safety, and reliability of the transportation system. Many intelligent transportation system solutions are part of TSM programs. AVs will optimize the use of existing roads and intersections by shortening gaps between cars, coordinating platoons, and employing more efficient route choices. However, cities may experience drawbacks when cars are left on their own to look for parking after they drop off their passengers. It is a well-known fact that a significant portion of traffic congestion in densely populated urban areas is caused by drivers looking for parking spaces. Because AVs have no need to find a parking space, this inconvenience and its resulting congestion will be reduced or eliminated in some areas. However, AVs will have to be sent to various destinations without any passengers. As the legendary urban designer Peter Calthorpe states, "the only thing worse than a single occupant vehicle (SOV) is a zero occupant vehicle (ZOV)" [8].

Another focus of TSM is optimizing incident clearance. Statistics reveal that driver error is the primary cause for all crashes [9]. Car accidents are not only a tragic safety issue; they also cause traffic congestion. Although confidence will take time to grow, with proper systems assurance and oversight, AVs will reduce—and eventually eliminate—human error and thus improve traffic safety. The congestion associated with accidents will diminish accordingly.

7. AV Impact on Tool 4: Improve Traffic by Widening Roadways and Adding New Roads and Parking

Conventional traffic engineering mistakenly treated roadway networks as conduits or pipelines, looking at them merely from the standpoint of supply and demand analysis without considering human factors. Since the 1950s, cities have given high priority to cars and roads rather than to people. Traffic congestion has increased, and walkable urban spaces have been compromised; the wider streets developed for cars are now considered unsafe and unappealing by pedestrians.

The "tragedy of commons" is an economic theory describing how individuals tend to act selfishly by depleting publicly accessible and underpriced or free resources, eventually degrading the public realm in terms of environment, energy consumption, health, and well-being. The theory is usually applied to the effects of pollution in public spaces, but the same principle can be seen in the way cars use public space. Travelers will continue to use and congest roads unless planning and policies—coupled with suitable design and land use measures—discourage private automobiles and provide incentives for public transit. A key question is whether AVs will result in more new and wider roads and parking spaces or whether they will result in the opposite.

The sizes and locations of parking facilities are expected to change significantly with the advent of AVs. Although a reduction in car ownership will decrease the need for parking facilities such as residential parking, park-and-ride sites, and shopping center parking, AVs will increase the need for dropoff spaces. Parking spaces for AV rentals may also increase in places such as public transit terminals and train stations [10].

Some studies and current projects advocate the segregation of AVs from human-operated vehicles. Dedicated guideways entail a wider right-of-way, wider curb radii at intersections, and potentially the provision of crash barriers, underpasses, or bridges. By widening roadways, segregation can compromise the walkability of a city. Typically, a pedestrian-friendly city will have few barriers, a narrower right-of-way, tighter corner radii at intersections to lower motorists' speed and a shared street system that allows different modes of transportation to coexist. However, at higher speeds, the need to build confidence in the safety of AVs remains a significant challenge before society allows a complete mixing of AVs with other vehicles on all roads. In the future, the need for segregated guideways will diminish, thus improving efficiency through the shared use of road infrastructure.

8. New Safety Challenges

Transportation systems face many new challenges in accommodating AVs. This paper focuses on the traffic demand and supply aspects of AVs; however, the impacts of AVs on safety, security, cost, energy consumption, pollution, privacy, and equity are also important. AVs could have both positive and negative effects on traffic and mobility. For example, AVs will enable many segments of the population (e.g., the elderly, the disabled, and those too young to drive) to become more mobile, which increases the number of people travelling and thus increases congestion.

AVs could greatly affect traffic safety. Todd Litman [11] comments that although AV optimists claim that 90 percent of crashes in the United States are attributable to human error and that accidents will decline overall, such claims overlook the fact that the convenience of AVs will put more vehicles on the road, and the added congestion is likely to increase accident rates. New safety risks will arise, such as hardware and software failures, malicious cyberattacks, or physical attacks on AVs for amusement, to test the system, or to prey on vulnerable people. AVs will provide greater mobility for the disabled, elderly, and younger passengers, enabling their greater inclusion in society, but they also present technical and safety challenges that must be addressed.

As confidence in AVs grows, passenger risk taking may also increase. AV passengers may use commuting time to eat, sleep, or exercise; as a result, they might cease to wear seatbelts. Pedestrians may use less caution walking in front of an AV than they would for a self-driven vehicle. During the early stages of AV deployment when self-driving vehicle are mixed with AVs, some drivers may attempt to join the platoons of AVs that may be operating on dedicated lanes close together at high speeds, which would result in increased crash severity. Furthermore, AVs have not been sufficiently tested in inclement weather (e.g., snow or heavy rain).

With the advent of AVs, the safety and security of both normal and vulnerable road users and pedestrians are challenges to be addressed. These issues will require further research followed by a rigorous and comprehensive approach to system assurance throughout the life cycle of AV development, testing, and operation. When system assurance is undertaken, the process should be broad enough to address the entire AV "ecosystem"; that is, the vehicles as well as all supporting and interfacing infrastructure that constitute the operating environment.

A key policy recommendation is for city leaders to quickly incorporate current efforts into the legal guidelines, specifications, rules, and safety regulations that are being developed for AVs worldwide.

9. Conclusion

Safety challenges notwithstanding, this paper focuses on how the four tools to relieve congestion must be revised to accommodate automated mobility. The following is a proposal for the key policy recommendations for each tool:

- Policy Recommendations for Tool 1: Land Use Measures
    1. *Ensure that compact, mixed-use developments (origins close to destinations) are preferred over spread-out, low-density city models to avoid the negative impact of widespread high usage of private AVs.*
    2. *Provide detailed policies to protect a city's urban growth boundary or green belt.*

- Policy Recommendations for Tool 2: TDM
    1. *Promote safe, high-quality public (shared) AV options to enable a modal shift away from SOVs or ZOVs.*
    2. *Provide subsidies for traveling in public AVs and provide disincentives for private AVs to move more people in a limited space.*

- Policy Recommendations for Tool 3: TSM
    1. *Develop AV safety regulations to enable AVs to coexist and integrate with normal traffic rather than limiting them to a specific guideway.*
    2. *Invest in connected traffic systems to ensure that AVs (a) navigate urban roads safely, (b) avoid traffic congestion, and (c) provide a bias for higher occupancy vehicles.*
    3. *Develop AVs in a manner that ensures they reduce and eventually avoid reliance on fossil fuels by integrating the latest electric vehicle and vehicle-to-grid smart energy storage systems.*

- Policy Recommendations for Tool 4: Road Widening/New Roads
    1. *Review all proposed road schemes in relation to AVs and the modal shift potential of public AVs.*
    2. *Review parking requirement standards in the light of the alternative requirements of AVs.*
    3. *Allocate space for strategically located AV charging and maintenance facilities.*
    4. *Design low-speed urban areas for the coexistence of AVs and pedestrians.*

With the advent of the automobile in the 20th century, some cities developed regulations and policies that resulted in positive impacts; others suffered. Such differences are reflected in the plans developed for New York by Robert Moses; in contrast was the position taken by the activist Jane Jacobs. Moses' decisions involved building highways and moving away from public transit, which resulted in urban sprawl and the far-flung suburbs of Long Island. However, Jane Jacobs organized grassroots efforts to protect neighborhoods from "slum clearance" — in particular, Moses' plans to overhaul Jacobs' own Greenwich Village neighborhood [12]. Moses' plan for the Lower Manhattan Expressway would have decimated the neighborhoods of SoHo and Little Italy; Jacobs was instrumental in the project's eventual cancellation. These neighborhoods experienced a renaissance in subsequent years.

Moses was a proponent of the early 20th-century vision that the only salvation of cities was the large-scale destruction of their existing features; Jacobs maintained that the future of cities rested on preserving those features. Jacobs' book, *The Death and Life of Great American Cities*, was a powerful rebuttal to Moses' mode of thinking, and her actions provided a convincing argument against his mode of operating [13].

Such dichotomies could also arise with the advent of automation in the 21st century; some cities may follow the Petropolis model to the detriment of their citizens and the planet as whole; while others will move toward the Ecopolis model. "Autonomous" should not be synonymous with "smart." If the substance of any action is smart, automation will make the system smarter. However, if the overall framework is not efficient, automation will exacerbate the inefficiencies. In conclusion, the challenge for municipalities and city leaders is to implement policy recommendations that bypass conventional transportation planning thinking to ensure that the advantages of AVs outweigh their potential disadvantages.

References

[1] Girardet, H. (2015). *Creating Regenerative Cities*. New York, NY: Routledge.

[2] Lay, M.G. (1992). *Ways of the World: A History of the World's Roads and of the Vehicles That Used Them.* New Brunswick, New Jersey: Rutgers University Press.

[3] Falcocchio, J.C., Levinson, H.S. (2015). *Road Traffic Congestion: A Concise Guide.* Chapter 2, How transportation technology has shaped urban travel patterns (pp. 9–17). Switzerland: Springer International Publishing.

[4] Kuzmyak, J.R., Caliper Corporation, PolyTech Corporation (2012). Land Use and Traffic Congestion, Final Report 618. Prepared for Arizona Department of Transportation Research Center, Arizona Department of Transportation in cooperation with U.S. Department of Transportation Federal Highway Administration.

[5] Alex, A. P., Saraswathy, M. V., Isaac, K. P. (2016). Latent variable enriched mode choice model for work activity in multi modal condition prevalent in India. *International Journal for Traffic and Transport Engineering,* 6(4), 378–389.

[6] Johansson, M.V., Heldt, T., Johansson, P. (2006). The effects of attitudes and personality traits on mode choice. *Transportation Research,* Part A 40, 507–525.

[7] Lubell, S. (2016). Here's How Self-Driving Cars Will Transform Your City. *Wired*, October 21. From https://www.wired.com/2016/10/heres-self-driving-cars-will-transform-city/

[8] Calthorpe, P., Walters, J. (2017). Autonomous Vehicles: Hype and Potential. *Urban Land*. Retrieved from https://urbanland.uli.org/industry-sectors/infrastructure-transit/autonomous-vehicles-hype-potential/

[9] National Highway Traffic Safety Administration (NHTSA), U.S. Department of Transportation (2008). Traffic Safety Facts 2008. A compilation of motor vehicle crash data from the fatality analysis reporting system and the general estimates system.

[10] Johnson, C. (2017). Readiness of the road network for connected and autonomous vehicles. RAC Foundation, London.

[11] Litman, T. (2018). Autonomous Vehicle Implementation Predictions. Victoria Transportation Policy Institute.

[12] Steyaert, J. (2012). Jane Jacobs, a Rebel with a Cause. Social Work and Society, Volume 10, Issue 1, 2012.

[13] Story of Cities #32: Jane Jacobs v Robert Moses, battle of New York's urban titans. (2016). The Guardian. https://www.theguardian.com/cities/2016/apr/28/story-cities-32-new-york-jane-jacobs-robert-moses?CMP=soc_568

Publication

Journal of Geotechnical and Transportation Engineering (JGTTE) is an Open Access journal accessible for free on the Internet. At JGTTE, we guarantee that no university library or individual reader will have to buy a subscription or pay any pay-per-view fees to access articles in the electronic version of the journal. There is hence no revenue at JGTTE neither from the sale of subscriptions to the electronic version of the journal nor from pay-per-view fees. Yet, the online publication process does involve costs including those pertaining to setup and maintenance of the publication infrastructure, routine operation of the journal, processing of manuscripts through peer-reviews, editing, publishing, maintaining the scholarly record, and archiving. To cover these costs, the journal depends on Article Process Charges, also called Publication Fees. This fee is due when a manuscript has been accepted for publication. There is an additional fee for the authors who are interested to receive a hard-copy of the journal in addition to the electronic version of the accepted papers. This additional fee is because of the printing and hard-copy publication, and shipment charges. Details of this fees are as follows:

Online Version	Hard Copy Plus Online	Subscription
$250	$350	$200 /annually
Permanent Access to the Link	Permanent Access to the Link	Hard copy of all issues
Free Indexing	Free Indexing	Permanent access to online issues
Free promotion service	Free promotion service	Conference affairs
Rapid Publication	Rapid Publication	Collaboration positions
Search Engine Friendly	Search Engine Friendly	Access to quarterly meetings

JGTTE does not request Article Submission Charges, also called Submission Fees. These are due at the time of submission of the manuscript. Nor JGTTE charge per page or for color figures or for any other items for the electronic version (e-version), for which other publishers are known to charge. The papers accepted for publication in e-version will be published online in full color without any extra charges. All the hard-copy versions will be in black and white. The authors who are interested that their paper be published in color in the hard-copy journal, can contact the publisher to discuss about this matter.

Please note that JGTTE's regular publication fees are well below average. All the while, JGTTE never ceases to seek to improve the quality guaranteed to its authors and its readers in all kinds of ways, including 1) generating article level metrics, 2) generating journal metrics, e.g., by calculating a 2-year Google-based Journal Impact Factor, and 3) archiving all articles at cloud. Authors should also keep in mind the cost effectiveness, or value for money, of publishing Open Access. JGTTE believes that it would score well on cost effectiveness.

Authors of an article are responsible for arranging the payment. That typically does not mean that authors end up paying for the publication of the article. The cost of the publication fee is very often assumed either by the organization funding the research, or by an Open Access Publishing Fund, or by the institution at which the author is employed.

Research funded by an agency that has an Open Access mandate will most probably cover the "publication fee" by the agency. For a database of Open Access mandates, please visit:

SHERPA JULIET

• Registry of Open Access Repositories Mandatory Archiving Policies (ROARMAP):Funder Mandates

Lists of Open Access Publishing Funds that could financially support your publication with JGTTE could be found at:

• Compact for Open-Access Publishing Equity: Signatories

• Open Access Directory: OA journal funds

• Scholarly Publishing and Academic Resources Coalition (SPARC): Open Access Funds (look under "Funds In Action")

• Co-Action Publishing: Institutes and Funders Covering Open Access Fees (APCs)

Please also approach your local university or organization to inquire about ways of supporting Open Access publication.

Contact:

New York / Los Angeles area:

m.Kamalzare@jgtte.com

1.646.580.4690

Washington, D.C. area:

h.Shabaniverki@jgtte.com

1.240.509.0038

General Request:

info@jgtte.com

Website:

www.jgtte.com

JGTTE

ISSN: 2379-8769| www.jgtte.com

ISSN 2379-8769

9 772379 876005

PUBLISHED IN USA

Volume 4 | Issue 1